Pseudomonas aeruginosa population dynamics in a vancomycin-induced murine model of gastrointestinal carriage

Marine Lebrun-Corbin[1], Bettina H. Cheung[1], Karthik Hullahalli[2,3], Katherine Dailey[2,3], Keith Bailey[4], Matthew K. Waldor[2,3], Richard G. Wunderink[5], Kelly E. R. Bachta[6], Alan R. Hauser[1,6]

1 - Department of Microbiology-Immunology, Feinberg School of Medicine, Northwestern University, Chicago, IL, USA

2 - Division of Infectious Disease, Brigham and Women's Hospital, Boston, MA, USA

3 - Department of Microbiology, Harvard Medical School, Boston, MA, USA

4 - Alnylam Pharmaceuticals, Cambridge, MA, USA

5 - Department of Medicine, Division of Pulmonary and Critical Care Medicine, Feinberg School of Medicine, Northwestern University, IL, USA

6 - Department of Medicine, Division of Infectious Diseases, Feinberg School of Medicine, Northwestern University, Chicago, IL, USA

ABSTRACT

Pseudomonas aeruginosa is a common nosocomial pathogen and a major cause of morbidity and mortality in hospitalized patients. Multiple reports highlight that *P. aeruginosa* gastrointestinal colonization may precede systemic infections by this pathogen. Gaining a deeper insight into the dynamics of *P. aeruginosa* gastrointestinal carriage is an essential step in managing gastrointestinal colonization and could contribute to preventing bacterial transmission and progression to systemic infection. Here, we present a clinically relevant mouse model relying on parenteral vancomycin pretreatment and a single orogastric gavage of a controlled dose of *P. aeruginosa.* Robust carriage was observed with multiple clinical isolates, and carriage persisted for up to 60 days. Histological and microbiological examination of mice indicated that this model indeed represented carriage and not infection. We then used a barcoded *P. aeruginosa* library along with the sequence tag-based analysis of microbial populations (STAMPR) analytic pipeline to quantify bacterial population dynamics and bottlenecks during the establishment of the gastrointestinal carriage. Analysis indicated that most of the *P. aeruginosa* population was rapidly eliminated in the stomach, but the few bacteria that moved to the small intestine and the caecum expanded significantly. Hence, the stomach constitutes a significant barrier against gastrointestinal carriage of *P. aeruginosa,* which may have clinical implications for hospitalized patients.

IMPORTANCE

While *P. aeruginosa* is rarely part of the normal human microbiome, carriage of the bacterium is quite frequent in hospitalized patients and residents of long-term care

facilities. *P. aeruginosa* carriage is a precursor to infection. Options for treating infections caused by difficult-to-treat *P. aeruginosa* strains are dwindling, underscoring the urgency to better understand and impede pre-infection stages, such as colonization. Here, we use vancomycin-treated mice to model antibiotic-treated patients who become colonized with *P. aeruginosa* in their gastrointestinal tracts. We identify the stomach as a major barrier to the establishment of gastrointestinal carriage. These findings suggest that efforts to prevent gastrointestinal colonization should focus not only on judicious use of antibiotics but also on investigation into how the stomach eliminates orally ingested *P. aeruginosa.*

INTRODUCTION

In 2019, one in eight global deaths were attributable to bacterial infections (1). A handful of bacteria were responsible for half of these deaths, including *Pseudomonas aeruginosa,* which causes a wide range of healthcare-associated infections such as pneumonia, bloodstream infections, wound or surgical site infections, and urinary tract infections (1, 2). These infections are especially life-threatening for individuals who are hospitalized, immunocompromised, or have chronic lung diseases. In addition to being one of the leading causes of nosocomial infections (3), *P. aeruginosa* is also highly resistant to antimicrobial agents, making these infections difficult to treat (4). Some *P. aeruginosa* isolates are resistant to nearly all available antibiotics, including carbapenems, which has led to the CDC classifying multidrug-resistant *P. aeruginosa* as a serious threat (5).

P. aeruginosa is rarely part of the gastrointestinal (GI) microbiome of healthy individuals (4%) (6); however, it more efficiently colonizes patients in the intensive care unit (ICU) (10-55%) (6–8), with cancer (31%-74% of hospitalized patients) (9, 10), or in long-term care facilities (52%) (11). Importantly, GI carriage of *P. aeruginosa* is a key risk factor for subsequent development of infection (7, 12–14). As part of a prospective study, Gómez-Zorrilla *et al*. determined that after a 14-day stay in the ICU the probability of developing a *P. aeruginosa* infection was 26% for carriers versus 5% for noncarriers (13). In addition to the risk for infection, GI carriage can facilitate transmission of *P. aeruginosa* to other patients (15, 16). Thus, gaining a deeper understanding of *P. aeruginosa* GI carriage is crucial to prevent infections, manage rising rates of antibiotic resistance, and improve overall patient safety in healthcare settings.

While several animal models are available for the investigation of *P. aeruginosa* virulence and dissemination (17–24), fewer models have focused on GI carriage. In patients, antibiotic use has been correlated with an increased risk of *P. aeruginosa* GI colonization (12, 25–27). Previous studies have exploited this correlation to develop animal models that have provided important information on how *P. aeruginosa* establishes carriage. However, these models have relied on extended exposure to *P. aeruginosa* or the use of immunocompromised mice (18, 28, 29). It is estimated that around two-thirds of patients in the ICU are immunocompetent (30, 31). By using antibiotic pretreatment and immunocompetent animals, we aimed to develop an animal model of *P. aeruginosa* GI carriage that better mimics a typical ICU patient.

Here, we describe a murine model of *P. aeruginosa* GI carriage that is facilitated by the daily intraperitoneal (IP) injection of vancomycin for seven days and by a single

dose of *P. aeruginosa* delivered via oral gavage. With this model, robust GI carriage was observed in both female and male mice, occurred with multiple clinical *P. aeruginosa* isolates, and persisted for up to 60 days. Additionally, to investigate the population dynamics of GI carriage, we used barcoded *P. aeruginosa* bacteria and determined that the stomach constituted a major barrier against GI carriage of *P. aeruginosa*. Bacteria that passed through the stomach were able to efficiently replicate in the small intestine and caecum, facilitating excretion of high numbers of *P. aeruginosa*. These barcoding experiments yielded interesting insights into the dynamics of *P. aeruginosa* GI carriage.

RESULTS

Vancomycin promotes gastrointestinal carriage of *P. aeruginosa*

Our goal was to develop a clinically relevant animal model that recapitulates the asymptomatic *P. aeruginosa* GI carriage observed in hospitalized patients. First, we tested the ability of the *P. aeruginosa* clinical isolate PABL048, delivered by orogastric gavage, to be carried in the GI tract of mice in the absence of antibiotic pretreatment. The extent of the carriage was assessed by fecal collection and plating on selective medium followed by CFU enumeration. Following pretreatment with IP phosphate-buffered saline (PBS), GI carriage of *P. aeruginosa* did not occur (Fig. 1A). Because antibiotic exposure correlates with an increased risk of GI colonization in patients (12, 25–27), we investigated the effect of IP vancomycin injection on the carriage of *P. aeruginosa* in mice. Vancomycin was chosen because it is one of the most commonly

used antibiotics in the U.S. (32, 33) and does not have activity against *P. aeruginosa* (34). Three regimens of IP vancomycin treatment combined with orogastric gavage of *P. aeruginosa* were tested (all with a daily dose of 370 mg/kg of vancomycin – equivalent to a human dose of 30 mg/kg (35)). All three regimens supported the carriage of *P. aeruginosa* (Supplemental Fig.1). While vancomycin pretreatment for either 3 or 5 days prior to the orogastric gavage led to similar levels of GI carriage of *P. aeruginosa,* higher fecal burdens were observed when vancomycin injections were continued for two days after the orogastric gavage (Supplemental Fig.1). For all subsequent experiments, we therefore chose a regimen consisting of vancomycin on days -4 to -1, vancomycin and *P. aeruginosa* on day 0, and vancomycin on days +1 and +2 (Fig. 1B), which cumulatively corresponds to a typical 7-day course of vancomycin commonly prescribed to patients (36). When mice were treated with this regimen of vancomycin and challenged with $10^{5.6}$ CFU of the *P. aeruginosa* isolate PABL048, bacterial shedding averaged 10^{6}-10^{8} CFU/g of feces during the first week (Fig. 1A). Although recovered CFU decreased somewhat during the second week post-inoculation, carriage levels remained between 10^{3} and 10^{7} CFU/g of feces. GI carriage of *P. aeruginosa* was similar in male and female mice (Fig. 1A).

A substantial proportion of the *P. aeruginosa* genome is accessory (i.e., varies from strain to strain) (37). To examine whether these genomic differences allowed some strains of *P. aeruginosa* to establish higher or lower levels of GI carriage in this model, we individually inoculated mice with six clinical isolates: PABL004, PABL006, PABL012, PABL048, PABL049 and PABL054. These isolates are genetically diverse and exhibit differing levels of virulence in a bloodstream infection model (38) (Supplementary Table

1). Despite these differences, bacterial loads detected in the feces were similar for all strains over the first 10 days of the experiment (Fig. 1C). While more variability was observed on day 14, persistent carriage of all strains was detected. These results, taken together with the establishment of GI carriage in both sexes, demonstrate that vancomycin pretreatment produces a robust and reliable model to investigate *P. aeruginosa* carriage.

GI carriage of *P. aeruginosa* does not cause GI inflammation

Carriage may be distinguished from infection by the absence of inflammation. To examine the vancomycin-treatment model represented true carriage, we performed histopathological analyses of the GI tract tissues. Mice received daily IP injections of vancomycin or PBS (day -4 to day +2) and were gavaged with either $10^{7.1}$ CFU of PABL048 or PBS (mock) on day 0. We chose to expose mice to a higher dose of bacteria than used in the previous experiments to maximize the possibility of observing inflammation. On day 3 post-orogastric gavage, mice were sacrificed and organs from the GI tract were harvested for histopathological examination. Organ sections were stained with hematoxylin-eosin (H&E) and screened for inflammation as evidenced by the presence of inflammatory cells or tissue damage. Neither of these were observed in any of the samples, and each section of the GI tract remained histologically normal (Fig. 2). Multifocal clusters of bacteria were observed adjacent to the mucosal surface of the stomach of all 3 mice that received IP PBS treatment and orogastric delivery of *P. aeruginosa.* These bacteria were primarily rod-shaped, compatible with *P. aeruginosa* morphology (39), but it was unclear whether they were dead or alive. Despite the

154 presence of these bacteria in the stomach of PBS-treated mice three days after
155 inoculation, *P. aeruginosa* bacteria were not cultured from their feces (Supplemental
156 Fig. 2). Among mice treated with vancomycin prior to the bacterial inoculation, only one
157 mouse exhibited bacteria adjacent to the surface mucosa of the stomach. While all mice
158 that received vancomycin treatment and *P. aeruginosa* had feces that grew this
159 bacterium (Supplemental Fig. 2), no bacteria were observed within the bowel walls of
160 the small intestine, the caecum, or the colon of these same animals (Fig. 2), suggesting
161 that *P. aeruginosa* remained in the lumen of the GI tract and did not invade the intestinal
162 wall. In addition to these histopathological observations, mice exhibited no signs of
163 systemic illness (e.g., decreased activity, ruffled fur) at any point during the experiment.
164 Taken together, these results suggest that this is a model of GI carriage of *P. aeruginosa*
165 rather than infection.
166
167 **_P. aeruginosa_ bacteria remain largely within the GI tract**
168 Since the intestinal tract has previously been identified as the main source of *P.*
169 *aeruginosa* for the development of infections in immunocompromised patients (12, 40,
170 41), we assessed whether this model resulted in dissemination of *P. aeruginosa* to other
171 tissues. Mice were orogastrically inoculated with $10^{7.4}$ CFU of PABL048, and *P.*
172 *aeruginosa* CFU were enumerated from various organs at days 3, 7 and 14 post
173 gavage. Most of the bacteria were detected in the organs of the GI tract, including the
174 stomach, small intestine, caecum, colon, and feces (Fig. 3). Nevertheless, *P.*
175 *aeruginosa* was occasionally detected in the gallbladder, spleen, liver, or lungs within
176 the first 7 days post gavage. This suggests that, in this model, escape of bacteria from

177 the gut, while very infrequent, did occasionally occur in the absence of observable signs
178 of systemic illness. However, by two weeks post-inoculation, we did not observe
179 bacteria in any systemic site of the mice. In summary, dissemination of *P. aeruginosa*
180 from the GI tract is rare in this model of GI carriage.
181
182 **_P. aeruginosa_ establishes long-term carriage**
183 To further characterize this model, we interrogated the duration of carriage
184 following a single orogastric gavage of *P. aeruginosa.* When inoculated with $10^{5.7}$ CFU
185 of PABL048, all mice carried *P. aeruginosa* in their GI tract for at least 10 days (Fig. 4).
186 At day 60, 70% of all mice (7/10 females, 7/10 males) were still shedding *P. aeruginosa*
187 from their GI tract. These results show that, in this model, *P. aeruginosa* establishes
188 long-term GI carriage following a single exposure.
189
190 **The stomach constitutes the main bottleneck of GI carriage**
191 Investigation across the segments of the GI tract indicated that not all tissues
192 supported the same levels of *P. aeruginosa* carriage (Fig. 3). Thus, we sought to
193 examine the GI carriage dynamics following orogastric inoculation with *P. aeruginosa.* In
194 particular, we wanted to identify which segments of the GI tract contributed to population
195 bottlenecks or supported bacterial expansion in this model. The sequence tag-based
196 analysis of microbial populations (STAMP) technique (42), which relies on the
197 generation of a bacterial library with insertions of short, random nucleotide DNA tags
198 into a neutral site of the chromosome, is ideal for this purpose. Animals are inoculated
199 with this library, and barcode frequency and diversity at different locations and times

post inoculation are interpreted using the refined framework of STAMP (known as "STAMPR") (43). This analysis estimates the size of the founding population (N_s), defined as the number of bacterial cells from the inoculum that successfully passed through physical, chemical and immune barriers in the host to establish the population at the site of infection. A low N_s value (a small number of unique barcodes) is indicative of a tight bottleneck, while a high N_s value (a large number of unique barcodes) is reflective of a wide bottleneck. Comparison of CFU obtained from a tissue with the N_s value provides insight into the extent of bacterial expansion; for example, high CFU could be obtained from 1) a wide bottleneck followed by little bacterial replication or 2) a tight bottleneck followed by extensive replication of a small number of founders.

We applied STAMP to the vancomycin-treated mouse model. We used a previously generated barcoded library in the *P. aeruginosa* clinical isolate PABL012 (~6,000 unique tags, each ~30 bp) that had been validated by Bachta and colleagues (designated "$PABL012_{pool}$") (44). Note that fecal shedding of PABL012 was similar to that of PABL048 in the vancomycin-treated mouse model (Fig. 1C). Because we observed stable GI carriage of PABL012 between days 3 and 7, we deduced that major steps of GI carriage establishment were likely to occur within the first 3 days following inoculation. Using the vancomycin-treated mouse model, we delivered $10^{6.1}$ CFU of the $PABL012_{pool}$ library through orogastric gavage and collected and analyzed segments of the GI tract (stomach, small intestine, caecum, colon, and feces) at 24, 48, or 72 hours post-inoculation (hpi).

As previously observed with PABL048 (Fig. 3), all organs of the GI tract supported the carriage of $PABL012_{pool}$ (Fig. 5A-D). The stomach was the organ with the

largest variation in total CFU recovered (Fig. 5 A-D); while *P. aeruginosa* was no longer recovered from the stomach of some mice, others carried 10^{4-5} CFU. The caecum and the feces had the highest bacterial burdens during the first 3 days of GI carriage. Median CFU loads recovered from all sites were stable over the first 3 days (Fig. 5D), suggesting that GI carriage is established during the first 24 hours following *P. aeruginosa* delivery and maintained for the next two days.

In all organs at all time points, N_s values were low, indicating that a tight bottleneck was encountered by *P. aeruginosa* following inoculation (Fig. 5A-C, E). N_s values were the lowest in the stomach, with median values below 10 for all three time points. Therefore, nearly all the bacteria initially inoculated into the stomach were either killed or expelled to the small intestine within the first 24 hours. The higher N_s values observed in the distal GI tract suggest that certain clones passed through the stomach but successfully established themselves further along the GI tract. By looking at the inoculum passage through the GI tract at early timepoints (1h and 6h post gavage), we confirmed that *P. aeruginosa* bacteria were mostly killed in the proximal GI tract rather than rapidly passaged to the distal GI tract and expelled in the feces (Supplemental Fig. 3). The nearly identical founding population sizes at each time point in the distal GI tract indicate that these segments are quite permissive for *P. aeruginosa* carriage (Fig. 5E). Taken together, these data suggest that nearly all *P. aeruginosa* bacteria are rapidly (in less than 6 hours) eliminated from the stomach and that a small number of bacteria pass through to the small intestine and downstream segments of the GI tract.

The small intestine and caecum support high replication of *P. aeruginosa*

246 The large CFU counts and corresponding small founding populations in different
247 organs highlighted the ability of *P. aeruginosa* to replicate in the GI tract (Fig. 5). For
248 each segment of the GI tract, we defined net replication (which includes the combined
249 effects of replication, death, and migration) as the ratio between CFU and N_s. The
250 greatest expansion of *P. aeruginosa* from a small founding population occurred in the
251 caecum with CFU/N_s ratio greater than 10^5, but substantial expansion was also
252 observed in the stomach, small intestine and colon (Supplemental Fig. 4). Theoretically,
253 high CFU/N_s could occur solely by local bacterial multiplication, by migration of bacteria
254 *en masse* from an adjacent portion of the GI tract, or a combination of these two
255 processes. Local multiplication would yield compartmentalized regions of the intestine,
256 where different clones are spatially segregated along the length of the GI tract. In
257 contrast, movement of bacterial populations along the GI tract would yield more similar
258 barcode distributions between regions of the intestine. To distinguish between these
259 possibilities, we quantified the genetic relatedness of *P. aeruginosa* populations in each
260 segment of the GI tract. Genetic relatedness is determined by comparing the genetic
261 distance (GD) of barcode distributions between two populations (45). GD varies from 0
262 to 0.9, with low values indicating highly similar barcode distributions between two
263 samples and high values indicating different barcode distributions between samples.
264 For all time points, the caecum, the colon, and the feces contained, on average, highly
265 similar barcode populations of *P. aeruginosa* (GD ≤ 0.06) (Fig. 6 A-D, dark purple).
266 Additionally, the GD between the small intestine and the caecum, colon and feces
267 decreased over time (Fig. 6D, teal). These findings, along with the high CFU/N_s values
268 observed in the distal GI tract (Supplemental Fig. 4), are consistent with a model in

which *P. aeruginosa,* despite not being viewed as an enteric bacterium, multiplies rapidly and to high numbers in the caecum or the small intestine. These large populations of bacteria then move to the colon and are subsequently expelled in the feces. They also support the conclusion that *P. aeruginosa* bacteria recovered from fecal samples are most representative of those carried in the distal GI tract and confirm the utility of using fecal sampling to study *P. aeruginosa* carriage.

Genetic similarity between two sites can be achieved through different population patterns. For example, two GI segments can be highly similar owing to a single dominant clone shared between both sites or due to underlying sharing of hundreds of clones, each with low abundance. To define the number of clones that contribute to genetic similarity, we calculated a metric known as “resilient” genetic distance (RD), which quantifies the number of shared clones that contribute to genetic similarity between two samples (0.8 threshold, see Methods) (43). Genetically similar samples with many shared clones have high RD values, whereas genetically similar samples which share only a few clones have low RD values.

The interpretation of whether RD is “low” or “high” is relative to the number of barcodes in a sample. To normalize RD values, the natural logarithm (ln) of RD is divided by the ln of the number of distinct barcodes, creating a fractional RD (FRD). The FRD represents the number of shared barcodes in a pair of samples (samples A and B) relative to the number of distinct barcodes in a reference sample (sample B) (43). For example, $FRD_{A\text{-}B}$ is calculated as $\frac{\ln(RD_{A-B}+1)}{\ln(Number\ of\ barcodes\ in\ B+1)}$, measuring the ratio of shared barcodes between samples A and B relative to the number of distinct barcodes in sample B. Therefore, an $FRD_{A\text{-}B}$ of ≈ 1 indicates that nearly all barcodes shared

between sample A and B are found in sample B, while low FRD_{A-B} indicates that shared clones represent a low fraction of barcodes in sample B. When contextualized with GD, FRD provides a normalized metric to interpret the number of shared clones that contribute to similarity and to suggest the possible directionality of clone transfer.

We next compared GD and FRD to decipher how clonal sharing of *P. aeruginosa* along the intestine changes over time. At 24 hpi, the *P. aeruginosa* populations in the stomach and the small intestine had only moderate similarity to those of the caecum, large intestine, and feces (average GDs = 0.54 and 0.41, respectively) (Fig. 6A). Using FRD values, we identified distinct patterns driving the genetic distances between the segments of the GI tract. At 24 hpi, the stomach and the small intestine had moderate genetic distance (average GD = 0.66) (Fig. 6A, D), indicating that the populations between these environments were relatively different. The median $FRD_{\text{stomach-small intestine}}$ (0.36) was lower than $FRD_{\text{small intestine-stomach}}$ (0.89) (Fig. 6H), illustrating that the shared barcodes constitute a smaller proportion of the total barcodes in the small intestine than in the stomach; the small intestine possesses a greater number of unique clones. The greater number of unique clones in the small intestine suggests either (1) reflux of a subpopulation of bacteria from the small intestine to the stomach or (2) initial seeding of the stomach and small intestine with more similar populations followed by rapid elimination of a portion of the population in the stomach. The decreasing GD between the stomach and the small intestine over time supports the idea of bacterial reflux from the small intestine. Very little similarity was present between *P. aeruginosa* populations in the feces and the stomach, indicating that coprophagia did not significantly contribute to reseeding of the stomach (Supplemental Fig. 5). Both the average $FRD_{\text{small intestine-}}$

315 $_{caecum}$ and $FRD_{caecum\text{-}small\ intestine}$ were greater than 0.9, indicating that relatedness
316 between the small intestine and caecum is driven by a large portion of shared barcodes
317 (Fig. 6E, H). The differential expansion of a small number of clones likely accounted for
318 the genetic distance (average GD = 0.41) between these two sites (Fig. 6A,
319 Supplemental Fig. 5). The high FRD and low GD values between the small intestine and
320 the caecum suggest that *P. aeruginosa* clones efficiently trafficked between these two
321 compartments, either through natural peristalsis or retrograde movement, before
322 continuing expansion at both sites. On the other hand, the extremely low GD values
323 between the caecum, colon, and feces (Fig. 6A-C) with corresponding FRD values ≥
324 0.89 (Fig. 6E-G) suggest that bacterial populations move freely between these sites.
325 These observations, together with the fact that CFU are consistently higher than N_s
326 values, indicate that vancomycin pretreatment robustly enables *P. aeruginosa*
327 replication and movement along the GI tract, rather than simply facilitating the transient
328 transfer of an initial inoculum through the GI tract.

329 Overall, our findings suggest that (i) the vast majority of orogastrically
330 administered *P. aeruginosa* bacteria are rapidly (within 6 hours) killed in the stomach, (ii)
331 less than 0.01% of *P. aeruginosa* from the inoculum persists in the intestine over the
332 first 72 hours, (iii) robust *P. aeruginosa* replication occurs in the small intestine and the
333 caecum, and (iv) bacterial populations subsequently migrate along the distal GI tract
334 and are expelled in the feces.
335

DISCUSSION

In this study, we established a murine model of *P. aeruginosa* GI carriage that mimics patients receiving antibiotics in the hospital setting. This model is clinically relevant, as it utilizes vancomycin, and has been validated with both sexes and multiple clinical isolates. The absence of GI tract inflammation confirmed that this model represents carriage, not infection. Nevertheless, occasional low-level escape of *P. aeruginosa* to other organs suggests a possible route by which GI carriage may lead to subsequent infection at remote sites (7, 12–14). Long-term GI carriage was established after a single dose of *P. aeruginosa*, with 70% of mice still carried the bacterium after 60 days. Using barcoded bacteria, we found that most of the bacterial inoculum was eliminated within the first 6 hours, primarily in the stomach. However, once *P. aeruginosa* reached the small intestine and the caecum, bacteria replicated robustly, leading to significant fecal excretion as winnowed bacterial populations migrated unimpeded through the caecum and colon.

Confirming previously reported results (28), we found that untreated mice did not support GI carriage of *P. aeruginosa.* In contrast, seven days of vancomycin delivered through IP injection promoted high-level and prolonged GI carriage of *P. aeruginosa*. Several studies have investigated the impact of orally administered vancomycin on the gut microbiota and have reported a decrease in *Bacteroidetes* and a subsequent increase in *Proteobacteria* and *Fusobacteria* phyla (46–50). *Firmicutes* levels were also altered by oral vancomycin treatments, with the directionality of the impact varying across bacterial species. We speculate that IP delivered vancomycin achieves relatively high concentrations in the lumen of the GI tract, that it has a similar effect on the mouse

359 microbiome, and that depletion of some microbiome constituents from the GI tract
360 creates a niche for the establishment of *P. aeruginosa*. While we did not observe
361 histopathological changes following vancomycin treatment, it is also possible that this
362 antibiotic facilitates *P. aeruginosa* carriage through a direct effect on the host, such as
363 immunomodulation, independent from a modification of the microbiome (49). As a first
364 step in understanding the mechanism by which vancomycin facilitates *P. aeruginosa*
365 carriage, we are currently characterizing the changes in the microbiome over time
366 following administration of vancomycin in this model.

367 All six clinical isolates of *P. aeruginosa* tested in our study established carriage in
368 the GI tract to a similar extent. These isolates are genetically diverse and include both
369 *exoU*$^{+}$ and *exoS*$^{+}$ strains, as well as high-risk and non-high-risk clones (38). Robust
370 colonization by different isolates suggests that the ability for *P. aeruginosa* to establish
371 GI carriage depends on a set of features encoded by the core genome of the bacterium.
372 Genes encoding metabolic factors, transcriptional regulators, adhesins, secretion
373 systems, membrane homeostasis proteins and bile resistance factors have been
374 identified as important for the GI carriage of other bacterial species (51–55). We
375 suspect that *P. aeruginosa* carriage requires a similar set of features. The reliance on
376 additional strain-specific strategies is nonetheless not excluded. Treatment with
377 vancomycin for seven days likely caused a severe dysbiosis, masking the need for
378 strain-specific factors that contribute to carriage in the presence of a less perturbed
379 microbiome. Additionally, we observed that GI carriage can last for several weeks
380 following a single exposure to the bacterium and cessation of vancomycin. Several
381 studies have reported that the long-term carriage of *P. aeruginosa* in the lungs of

382 individuals with cystic fibrosis or chronic obstructive pulmonary disease is accompanied
383 by genetic adaptations of the bacterium (56–58). It is possible that the set of genes or
384 alleles contributing to carriage of *P. aeruginosa* evolves as bacteria transition from the
385 early stages of carriage to long-term colonization.

386 In patients, the GI carriage of *P. aeruginosa* is a predictor for the subsequent
387 development of *P. aeruginosa* infections at various sites (7, 12, 13). Shortly after
388 bacterial inoculation, we show that low-level dissemination from the gut to the
389 gallbladder, spleen, liver, or lungs occasionally occurs, perhaps explaining these clinical
390 observations. Gut dysbiosis can lead to the development of a leaky intestinal barrier,
391 where pathogen molecules translocate from the gut into the bloodstream (59). The
392 present study utilized healthy mice. However, dissemination to other tissues may be
393 accentuated in immunocompromised animals, leading to more severe infections, as
394 shown by Koh *et al.* (18). Interestingly, 12 days after cessation of vancomycin
395 administration (14 days after orogastric gavage with *P. aeruginosa*), *P. aeruginosa* CFU
396 in the feces remained high but dissemination from the gut was no longer observed.
397 Calderon-Gonzalez *et al.* showed that *Klebsiella pneumoniae* dissemination from the GI
398 tract was promoted by antibiotic treatments (51). It is therefore possible that vancomycin
399 may support not only GI carriage but also dissemination of *P. aeruginosa,* and that
400 dissemination diminishes over time as vancomycin is cleared.

401 STAMPR has been used by several groups to measure the dynamics of bacterial
402 spread in colonization and systemic dissemination (44, 60, 61). We used STAMPR to
403 show that most *P. aeruginosa* bacteria are eradicated prior to carriage. Two recent
404 studies indicate that stomach acidity significantly restricts the GI carriage of *Citrobacter*

rodentium and *K. pneumoniae* (51, 62). While stomach acidity constricts *C. rodentium* numbers by 10- to 100-fold (62), our results show an even more severe constriction for *P. aeruginosa* in the stomach. The stomach pH of healthy mice fluctuates between 3-4, while the rest of the GI tract tends to have a more neutral pH of 6-8 (63). *P. aeruginosa* can grow at a wide range of pH, but its optimal growth pH ranges between 6 and 8 (64). Thus, acidity may be the mechanism underlying the loss of *P. aeruginosa* barcode diversity in the stomach. This possibility could be tested by pharmacologically neutralizing stomach acid and subsequently measuring the size of downstream founding populations of *P. aeruginosa.* Interestingly, the rest of the GI tract was quite permissive to carriage. In the absence of vancomycin treatment, no carriage could be established, indicating the presence of a second barrier to *P. aeruginosa,* perhaps downstream of the stomach in untreated mice. Campbell *et al.* recently monitored the dynamics of *C. rodentium* enteric carriage and identified the microbiota as the major factor limiting colonization (62). This supports the idea that vancomycin facilitates the carriage of *P. aeruginosa* by eliminating a microbiome-mediated barrier, a hypothesis that could be tested with germ-free mice. In this sense, *P. aeruginosa* is both an "opportunistic pathogen" and an "opportunistic colonizer."

Together, our findings suggest the following model of *P. aeruginosa* carriage: within a few hours (less than 6 hours), a drastic constriction (less than 0.01% survival on average) of the bacterial inoculum occurs in the stomach (Fig. 7). A very small proportion of the *P. aeruginosa* inoculum passes through the stomach to reach the small intestine and the caecum. The small number of remaining founders rapidly replicate in both the small intestine and the caecum, and the resulting bacterial populations migrate

from the caecum to the colon and are expelled in the feces. In addition to the expected trafficking route from the stomach to the small intestine, a small portion of *P. aeruginosa* may also reflux from the small intestine back to the stomach. Using STAMPR, we have identified the stomach as the main barrier to *P. aeruginosa* carriage in this animal model and the small intestine and the caecum as the main sites of bacterial expansion. Overall, this model advances the understanding of *P. aeruginosa* dynamics during GI carriage and may be useful in studying adaptation of *P. aeruginosa* during prolonged colonization, persistence following administration of antibiotics other than vancomycin, and identification of *P. aeruginosa* and host factors that facilitate carriage. In addition, our findings have clinical implications, such as the potential importance of more judicious use of acid suppressing drugs and vancomycin in preventing *P. aeruginosa* GI carriage.

MATERIALS AND METHODS

Bacterial strains and culture conditions

PABL004, PABL006, PABL012, PABL048, PABL049 and PABL054 are archived *P. aeruginosa* clinical isolates cultured between 1999 and 2003 from the bloodstream of patients at Northwestern Memorial Hospital in Chicago (65). Relevant characteristics of the strains are listed in Supplementary Table 1. Unless otherwise stated, bacteria were streaked from frozen stocks onto either Lysogeny broth (LB) or Vogel-Bonner minimal (VBM) (66) agar plates and subsequently grown at 37°C in LB medium with shaking.

When antibiotic selection for *P. aeruginosa* was necessary, supplementation with irgasan (irg) at 5 µg/mL was used.

Murine model of gastrointestinal carriage

Six- to eight-week-old C57BL/6 mice (Jackson Laboratory) received either 200 µL (female) or 250 µL (male) of vancomycin (370 mg/kg, Hospira, Lake Forest, IL) daily IP for seven days. The vancomycin dosage was allometrically scaled based on a total human daily dose of 30 mg/kg (35). On the fifth day of antibiotic treatment, mice were gavaged (20 G x 30 mm straight animal feeding needle, Pet Surgical, Phoenix, AZ) with 50 µL of *P. aeruginosa* prepared as follows: after overnight culture in LB, bacteria were diluted, regrown to exponential phase in LB and resuspended to the desired dose in PBS. When specified, mock IP injections or mock orogastric gavage was performed using PBS (same volumes as the treatment groups). Starting the day after the orogastric gavage, cages were changed daily to limit the impact of coprophagy.

To determine bacterial GI carriage, mice were individually placed in boxes to induce defecation, and feces were collected, weighed, homogenized in 1 mL of PBS using a bead blaster (Benchmark Scientific, Sayreville, NJ), and centrifuged for 30 sec at 1,100 x *g*. The supernatant was serially diluted and plated on either LB agar supplemented with irgasan or VBM agar for CFU enumeration.

Mice were housed in the containment ward of the Center for Comparative Medicine at Northwestern University. All experiments were approved by the Northwestern University Institutional Animal Care and Use Committee in compliance

with all relevant ethical regulations for animal testing and research. Experiments used female mice unless otherwise stated.

Murine GI carriage of PABL012$_{pool}$

Six- to eight-week-old female mice received IP injection of vancomycin (200 µL, 370 mg/kg) for 5 to 7 days, with each experimental group receiving their last injection 24 h prior to dissection. An aliquot of 50 µL of the PABL012$_{pool}$ library was grown overnight in 5 mL of LB (37°C, 250 rpm) and subcultured (1:40) in 30 mL of LB for 3 h. The bacterial inoculum was prepared as described above, and orogastric gavage was performed on the 5th day of vancomycin treatment, using $10^{6.1}$ CFU of PABL012$_{pool}$. Following bacterial inoculation, mice were housed individually. At 24, 48, and 72 hours post-gavage, mice were euthanized, and the stomach, small intestine, caecum, colon and feces were collected. The stomach, small intestine and caecum were processed along with their luminal contents. The colon was emptied, and the colonic contents were added to excreted feces (when available) to constitute the “feces” samples. All samples were weighed, homogenized in 1 mL of PBS using a bead blaster, centrifuged for 30 sec at 1,100 x *g*, and the supernatant was serially diluted and plated on VBM agar for CFU enumeration. For the estimated founding population sizes (N_s), 250 µL of the organ samples, as well as 250 µL of the inoculum (26 technical replicates) were spread on 150-mm-diameter VBM plates. Plates used for CFU and N_s determination were grown overnight at 37°C and the colonies were counted. CFU counts and N_s values in figure 5 represent those determined in 250 µL (1/4 of the homogenized tissue volume).

ACKNOWLEDMENTS

Support for this work was provided by the National Institutes of Health awards RO1 AI118257, K24 AI04831, R21 AI129167 and R21 AI153953 (all to ARH) and U19 AI135964 (RGW and ARH). Histology services were provided by the Northwestern University Mouse Histology and Phenotyping Laboratory which is supported by NCI P30-CA060553 awarded to the Robert H Lurie Comprehensive Cancer Center.

REFERENCES

1. Ikuta KS, Swetschinski LR, Aguilar GR, Sharara F, Mestrovic T, Gray AP, Weaver ND, Wool EE, Han C, Hayoon AG, Aali A, Abate SM, Abbasi-Kangevari M, Abbasi-Kangevari Z, Abd-Elsalam S, Abebe G, Abedi A, Abhari AP, Abidi H, Aboagye RG, Absalan A, Ali HA, Acuna JM, Adane TD, Addo IY, Adegboye OA, Adnan M, Adnani QES, Afzal MS, Afzal S, Aghdam ZB, Ahinkorah BO, Ahmad A, Ahmad AR, Ahmad R, Ahmad S, Ahmad S, Ahmadi S, Ahmed A, Ahmed H, Ahmed JQ, Rashid TA, Ajami M, Aji B, Akbarzadeh-Khiavi M, Akunna CJ, Hamad HA, Alahdab F, Al-Aly Z, Aldeyab MA, Aleman AV, Alhalaiqa FAN, Alhassan RK, Ali BA, Ali L, Ali SS, Alimohamadi Y, Alipour V, Alizadeh A, Aljunid SM, Allel K, Almustanyir S, Ameyaw EK, Amit AML, Anandavelane N, Ancuceanu R, Andrei CL, Andrei T, Anggraini D, Ansar A, Anyasodor AE, Arabloo J, Aravkin AY, Areda D, Aripov T, Artamonov AA, Arulappan J, Aruleba RT, Asaduzzaman M, Ashraf T, Athari SS, Atlaw D, Attia S, Ausloos M, Awoke T, Quintanilla BPA, Ayana TM, Azadnajafabad S, Jafari AA, B DB, Badar M, Badiye AD, Baghcheghi N, Bagherieh S, Baig AA, Banerjee I, Barac A, Bardhan M, Barone-Adesi F, Barqawi HJ, Barrow A, Baskaran P, Basu S, Batiha A-MM, Bedi N, Belete MA, Belgaumi UI,

517 Bender RG, Bhandari B, Bhandari D, Bhardwaj P, Bhaskar S, Bhattacharyya K, Bhattarai S,
518 Bitaraf S, Buonsenso D, Butt ZA, Santos FLC dos, Cai J, Calina D, Camargos P, Cámera LA,
519 Cárdenas R, Cevik M, Chadwick J, Charan J, Chaurasia A, Ching PR, Choudhari SG,
520 Chowdhury EK, Chowdhury FR, Chu D-T, Chukwu IS, Dadras O, Dagnaw FT, Dai X, Das S,
521 Dastiridou A, Debela SA, Demisse FW, Demissie S, Dereje D, Derese M, Desai HD, Dessalegn
522 FN, Dessalegni SAA, Desye B, Dhaduk K, Dhimal M, Dhingra S, Diao N, Diaz D, Djalalinia S,
523 Dodangeh M, Dongarwar D, Dora BT, Dorostkar F, Dsouza HL, Dubljanin E, Dunachie SJ,
524 Durojaiye OC, Edinur HA, Ejigu HB, Ekholuenetale M, Ekundayo TC, El-Abid H, Elhadi M,
525 Elmonem MA, Emami A, Bain LE, Enyew DB, Erkhembayar R, Eshrati B, Etaee F, Fagbamigbe
526 AF, Falahi S, Fallahzadeh A, Faraon EJA, Fatehizadeh A, Fekadu G, Fernandes JC, Ferrari A,
527 Fetensa G, Filip I, Fischer F, Foroutan M, Gaal PA, Gadanya MA, Gaidhane AM, Ganesan B,
528 Gebrehiwot M, Ghanbari R, Nour MG, Ghashghaee A, Gholamrezanezhad A, Gholizadeh A,
529 Golechha M, Goleij P, Golinelli D, Goodridge A, Gunawardane DA, Guo Y, Gupta RD, Gupta
530 S, Gupta VB, Gupta VK, Guta A, Habibzadeh P, Avval AH, Halwani R, Hanif A, Hannan MA,
531 Harapan H, Hassan S, Hassankhani H, Hayat K, Heibati B, Heidari G, Heidari M, Heidari-
532 Soureshjani R, Herteliu C, Heyi DZ, Hezam K, Hoogar P, Horita N, Hossain MM,
533 Hosseinzadeh M, Hostiuc M, Hostiuc S, Hoveidamanesh S, Huang J, Hussain S, Hussein NR,
534 Ibitoye SE, Ilesanmi OS, Ilic IM, Ilic MD, Imam MT, Immurana M, Inbaraj LR, Iradukunda A,
535 Ismail NE, Iwu CCD, Iwu CJ, J LM, Jakovljevic M, Jamshidi E, Javaheri T, Javanmardi F,
536 Javidnia J, Jayapal SK, Jayarajah U, Jebai R, Jha RP, Joo T, Joseph N, Joukar F, Jozwiak JJ,
537 Kacimi SEO, Kadashetti V, Kalankesh LR, Kalhor R, Kamal VK, Kandel H, Kapoor N, Karkhah S,
538 Kassa BG, Kassebaum NJ, Katoto PD, Keykhaei M, Khajuria H, Khan A, Khan IA, Khan M,

539 Khan MN, Khan MA, Khatatbeh MM, Khater MM, Kashani HRK, Khubchandani J, Kim H, Kim
540 MS, Kimokoti RW, Kissoon N, Kochhar S, Kompani F, Kosen S, Koul PA, Laxminarayana SLK,
541 Lopez FK, Krishan K, Krishnamoorthy V, Kulkarni V, Kumar N, Kurmi OP, Kuttikkattu A, Kyu
542 HH, Lal DK, Lám J, Landires I, Lasrado S, Lee S, Lenzi J, Lewycka S, Li S, Lim SS, Liu W, Lodha
543 R, Loftus MJ, Lohiya A, Lorenzovici L, Lotfi M, Mahmoodpoor A, Mahmoud MA, Mahmoudi
544 R, Majeed A, Majidpoor J, Makki A, Mamo GA, Manla Y, Martorell M, Matei CN, McManigal
545 B, Nasab EM, Mehrotra R, Melese A, Mendoza-Cano O, Menezes RG, Mentis A-FA, Micha
546 G, Michalek IM, Sá ACMGN de, Kostova NM, Mir SA, Mirghafourvand M, Mirmoeeni S,
547 Mirrakhimov EM, Mirza-Aghazadeh-Attari M, Misganaw AS, Misganaw A, Misra S,
548 Mohammadi E, Mohammadi M, Mohammadian-Hafshejani A, Mohammed S, Mohan S,
549 Mohseni M, Mokdad AH, Momtazmanesh S, Monasta L, Moore CE, Moradi M, Sarabi MM,
550 Morrison SD, Motaghinejad M, Isfahani HM, Khaneghah AM, Mousavi-Aghdas SA, Mubarik
551 S, Mulita F, Mulu GBB, Munro SB, Muthupandian S, Nair TS, Naqvi AA, Narang H, Natto ZS,
552 Naveed M, Nayak BP, Naz S, Negoi I, Nejadghaderi SA, Kandel SN, Ngwa CH, Niazi RK, Sá
553 ATN de, Noroozi N, Nouraei H, Nowroozi A, Nuñez-Samudio V, Nutor JJ, Nzoputam CI,
554 Nzoputam OJ, Oancea B, Obaidur RM, Ojha VA, Okekunle AP, Okonji OC, Olagunju AT,
555 Olusanya BO, Bali AO, Omer E, Otstavnov N, Oumer B, A MP, Padubidri JR, Pakshir K, Palicz
556 T, Pana A, Pardhan S, Paredes JL, Parekh U, Park E-C, Park S, Pathak A, Paudel R, Paudel U,
557 Pawar S, Toroudi HP, Peng M, Pensato U, Pepito VCF, Pereira M, Peres MFP, Perico N, Petcu
558 I-R, Piracha ZZ, Podder I, Pokhrel N, Poluru R, Postma MJ, Pourtaheri N, Prashant A, Qattea
559 I, Rabiee M, Rabiee N, Radfar A, Raeghi S, Rafiei S, Raghav PR, Rahbarnia L, Rahimi-
560 Movaghar V, Rahman M, Rahman MA, Rahmani AM, Rahmanian V, Ram P, Ranjha MMAN,

561 Rao SJ, Rashidi M-M, Rasul A, Ratan ZA, Rawaf S, Rawassizadeh R, Razeghinia MS, Redwan
562 EMM, Regasa MT, Remuzzi G, Reta MA, Rezaei N, Rezapour A, Riad A, Ripon RK, Rudd KE,
563 Saddik B, Sadeghian S, Saeed U, Safaei M, Safary A, Safi SZ, Sahebazzamani M, Sahebkar A,
564 Sahoo H, Salahi S, Salahi S, Salari H, Salehi S, Kafil HS, Samy AM, Sanadgol N, Sankararaman
565 S, Sanmarchi F, Sathian B, Sawhney M, Saya GK, Senthilkumaran S, Seylani A, Shah PA,
566 Shaikh MA, Shaker E, Shakhmardanov MZ, Sharew MM, Sharifi-Razavi A, Sharma P, Sheikhi
567 RA, Sheikhy A, Shetty PH, Shigematsu M, Shin JI, Shirzad-Aski H, Shivakumar KM, Shobeiri
568 P, Shorofi SA, Shrestha S, Sibhat MM, Sidemo NB, Sikder MK, Silva LMLR, Singh JA, Singh P,
569 Singh S, Siraj MS, Siwal SS, Skryabin VY, Skryabina AA, Socea B, Solomon DD, Song Y,
570 Sreeramareddy CT, Suleman M, Abdulkader RS, Sultana S, Szócska M, Tabatabaeizadeh S-A,
571 Tabish M, Taheri M, Taki E, Tan K-K, Tandukar S, Tat NY, Tat VY, Tefera BN, Tefera YM,
572 Temesgen G, Temsah M-H, Tharwat S, Thiyagarajan A, Tleyjeh II, Troeger CE, Umapathi KK,
573 Upadhyay E, Tahbaz SV, Valdez PR, Eynde JV den, Doorn HR van, Vaziri S, Verras G-I,
574 Viswanathan H, Vo B, Waris A, Wassie GT, Wickramasinghe ND, Yaghoubi S, Yahya GATY,
575 Jabbari SHY, Yigit A, Yiğit V, Yon DK, Yonemoto N, Zahir M, Zaman BA, Zaman SB,
576 Zangiabadian M, Zare I, Zastrozhin MS, Zhang Z-J, Zheng P, Zhong C, Zoladl M, Zumla A, Hay
577 SI, Dolecek C, Sartorius B, Murray CJL, Naghavi M. 2022. Global mortality associated with
578 33 bacterial pathogens in 2019: a systematic analysis for the Global Burden of Disease
579 Study 2019. The Lancet 400:2221–2248.

580 2. Centers for the Disease Control and Prevention. 2023. *Pseudomonas aeruginosa* Infection |
581 HAI | CDC. https://www.cdc.gov/hai/organisms/pseudomonas.html. Retrieved 8 March
582 2024.

583 3. Magill SS, Edwards JR, Bamberg W, Beldavs ZG, Dumyati G, Kainer MA, Lynfield R, Maloney
584 M, McAllister-Hollod L, Nadle J, Ray SM, Thompson DL, Wilson LE, Fridkin SK, Emerging
585 Infections Program Healthcare-Associated Infections and Antimicrobial Use Prevalence
586 Survey Team. 2014. Multistate point-prevalence survey of health care-associated
587 infections. N Engl J Med 370:1198–1208.

588 4. Boucher HW, Talbot GH, Bradley JS, Edwards JE, Gilbert D, Rice LB, Scheld M, Spellberg B,
589 Bartlett J. 2009. Bad Bugs, No Drugs: No ESKAPE! An Update from the Infectious Diseases
590 Society of America. Clin Infect Dis 48:1–12.

591 5. Centers for Disease Control and Prevention (U.S.). 2019. Antibiotic resistance threats in the
592 United States, 2019. Centers for Disease Control and Prevention (U.S.).

593 6. Hu Y, Wang S, Zhang Y, Wu Y, Liu C, Ju X, Zhou H, Cai C, Zhang R. 2023. A comparative study
594 of intestinal *Pseudomonas aeruginosa* in healthy individuals and ICU inpatients. One
595 Health Adv 1:13.

596 7. Cohen R, Babushkin F, Cohen S, Afraimov M, Shapiro M, Uda M, Khabra E, Adler A, Ben Ami
597 R, Paikin S. 2017. A prospective survey of *Pseudomonas aeruginosa* colonization and
598 infection in the intensive care unit. Antimicrob Resist Infect Control 6:7.

599 8. Gómez-Zorrilla S, Camoez M, Tubau F, Periche E, Cañizares R, Dominguez MA, Ariza J, Peña
600 C. 2014. Antibiotic Pressure Is a Major Risk Factor for Rectal Colonization by Multidrug-
601 Resistant *Pseudomonas aeruginosa* in Critically Ill Patients. Antimicrob Agents Chemother
602 58:5863–5870.

603 9. Andremont A, Marang B, Tancrède C, Baume D, Hill C. 1989. Antibiotic treatment and
604 intestinal colonization by *Pseudomonas aeruginosa* in cancer patients. Antimicrob Agents
605 Chemother 33:1400–1402.

606 10. Willmann M, Klimek AM, Vogel W, Liese J, Marschal M, Autenrieth IB, Peter S, Buhl M.
607 2014. Clinical and treatment-related risk factors for nosocomial colonisation with
608 extensively drug-resistant *Pseudomonas aeruginosa* in a haematological patient
609 population: a matched case control study. BMC Infect Dis 14.

610 11. Martak D, Gbaguidi-Haore H, Meunier A, Valot B, Conzelmann N, Eib M, Autenrieth IB,
611 Slekovec C, Tacconelli E, Bertrand X, Peter S, Hocquet D, Guther J. 2022. High prevalence of
612 *Pseudomonas aeruginosa* carriage in residents of French and German long-term care
613 facilities. Clin Microbiol Infect 28:1353–1358.

614 12. Ohara T, Itoh K. 2003. Significance of *Pseudomonas aeruginosa* Colonization of the
615 Gastrointestinal Tract. Intern Med 42:1072–1076.

616 13. Gómez-Zorrilla S, Camoez M, Tubau F, Cañizares R, Periche E, Dominguez MA, Ariza J, Peña
617 C. 2015. Prospective Observational Study of Prior Rectal Colonization Status as a Predictor
618 for Subsequent Development of *Pseudomonas aeruginosa* Clinical Infections. Antimicrob
619 Agents Chemother 59:5213–5219.

620 14. Wheatley RM, Caballero JD, van der Schalk TE, De Winter FHR, Shaw LP, Kapel N, Recanatini
621 C, Timbermont L, Kluytmans J, Esser M, Lacoma A, Prat-Aymerich C, Oliver A, Kumar-Singh
622 S, Malhotra-Kumar S, Craig MacLean R. 2022. Gut to lung translocation and antibiotic

623 mediated selection shape the dynamics of *Pseudomonas aeruginosa* in an ICU patient. 1.
624 Nat Commun 13:6523.

625 15. Denton M, Kerr K, Mooney L, Keer V, Rajgopal A, Brownlee K, Arundel P, Conway S. 2002.
626 Transmission of colistin-resistant *Pseudomonas aeruginosa* between patients attending a
627 pediatric cystic fibrosis center. Pediatr Pulmonol 34:257–261.

628 16. Bertrand X, Thouverez M, Talon D, Boillot A, Capellier G, Floriot C, Hélias J. 2001.
629 Endemicity, molecular diversity and colonisation routes of Pseudomonas aeruginosa in
630 intensive care units. Intensive Care Med 27:1263–1268.

631 17. Comolli JC, Hauser AR, Waite L, Whitchurch CB, Mattick JS, Engel JN. 1999. *Pseudomonas*
632 *aeruginosa* gene products PilT and PilU are required for cytotoxicity in vitro and virulence
633 in a mouse model of acute pneumonia. Infect Immun 67:3625–3630.

634 18. Koh AY, Priebe GP, Pier GB. 2005. Virulence of *Pseudomonas aeruginosa* in a Murine Model
635 of Gastrointestinal Colonization and Dissemination in Neutropenia. Infect Immun 73:2262–
636 2272.

637 19. Cash HA, Woods DE, McCullough B, Johanson WG, Bass JA. 1979. A rat model of chronic
638 respiratory infection with *Pseudomonas aeruginosa*. Am Rev Respir Dis 119:453–459.

639 20. van Heeckeren AM, Schluchter MD. 2002. Murine models of chronic *Pseudomonas*
640 *aeruginosa* lung infection. Lab Anim 36:291–312.

641 21. Cole N, Bao S, Stapleton F, Thakur A, Husband AJ, Beagley KW, Willcox MDP. 2003.
642 *Pseudomonas aeruginosa* keratitis in IL-6-deficient mice. Int Arch Allergy Immunol
643 130:165–172.

644 22. Wood SJ, Kuzel TM, Shafikhani SH. 2023. *Pseudomonas aeruginosa*: Infections, Animal
645 Modeling, and Therapeutics. 1. Cells 12:199.

646 23. Goldufsky J, Wood SJ, Jayaraman V, Majdobeh O, Chen L, Qin S, Zhang C, DiPietro LA,
647 Shafikhani SH. 2015. *Pseudomonas aeruginosa* uses T3SS to inhibit diabetic wound healing.
648 Wound Repair Regen 23:557–564.

649 24. Pennington JE, Ehrie MG. 1978. Pathogenesis of *Pseudomonas aeruginosa* pneumonia
650 during immunosuppression. J Infect Dis 137:764–774.

651 25. Pettigrew MM, Gent JF, Kong Y, Halpin AL, Pineles L, Harris AD, Johnson JK. 2019.
652 Gastrointestinal Microbiota Disruption and Risk of Colonization With Carbapenem-
653 resistant *Pseudomonas aeruginosa* in Intensive Care Unit Patients. Clin Infect Dis 69:604–
654 613.

655 26. Lepelletier D, Caroff N, Riochet D, Bizouarn P, Bourdeau A, Le Gallou F, Espaze E, Reynaud
656 A, Richet H. 2006. Role of hospital stay and antibiotic use on *Pseudomonas aeruginosa*
657 gastrointestinal colonization in hospitalized patients. Eur J Clin Microbiol Infect Dis 25:600–
658 603.

659 27. Hoang S, Georget A, Asselineau J, Venier A-G, Leroyer C, Rogues AM, Thiébaut R. 2018. Risk
660 factors for colonization and infection by *Pseudomonas aeruginosa* in patients hospitalized
661 in intensive care units in France. PLoS ONE 13:e0193300.

662 28. Pier GB, Meluleni G, Neuger E. 1992. A murine model of chronic mucosal colonization by
663 *Pseudomonas aeruginosa*. Infect Immun 60:4768–4776.

664 29. Janapatla RP, Dudek A, Chen C-L, Chuang C-H, Chien K-Y, Feng Y, Yeh Y-M, Wang Y-H, Chang
665 H-J, Lee Y-C, Chiu C-H. 2023. Marine prebiotics mediate decolonization of *Pseudomonas*
666 *aeruginosa* from gut by inhibiting secreted virulence factor interactions with mucins and
667 enriching Bacteroides population. J Biomed Sci 30:9.

668 30. Zebian G, Kreitmann L, Houard M, Piantoni A, Piga G, Ruffier des Aimes S, Holik B, Wallet F,
669 Labreuche J, Nseir S. 2024. Immunosuppression at ICU admission is not associated with a
670 higher incidence of ICU-acquired bacterial bloodstream infections: the COCONUT study.
671 Ann Intensive Care 14:83.

672 31. Kreitmann L, Helms J, Martin-Loeches I, Salluh J, Poulakou G, Pène F, Nseir S. 2024. ICU-
673 acquired infections in immunocompromised patients. Intensive Care Med 50:332–349.

674 32. Baggs J, Fridkin SK, Pollack LA, Srinivasan A, Jernigan JA. 2016. Estimating National Trends
675 in Inpatient Antibiotic Use Among US Hospitals From 2006 to 2012. JAMA Intern Med
676 176:1639–1648.

677 33. Magill SS, O'Leary E, Ray SM, Kainer MA, Evans C, Bamberg WM, Johnston H, Janelle SJ,
678 Oyewumi T, Lynfield R, Rainbow J, Warnke L, Nadle J, Thompson DL, Sharmin S, Pierce R,

679 Zhang AY, Ocampo V, Maloney M, Greissman S, Wilson LE, Dumyati G, Edwards JR,
680 Emerging Infections Program Hospital Prevalence Survey Team. 2021. Antimicrobial Use in
681 US Hospitals: Comparison of Results From Emerging Infections Program Prevalence
682 Surveys, 2015 and 2011. Clin Infect Dis 72:1784–1792.

683 34. Hauser AR. 2018. Antibiotic Basics for Clinicians: The ABCs of Choosing the Right
684 Antibacterial Agent, 3rd ed. Lippincott Williams & Wilkins (LWW).

685 35. U.S. Department of Health and Human Services. 2005. Guidance for Industry - Estimating
686 the Maximum Safe Starting Dose in Initial Clinical Trials for Therapeutics in Adult Healthy
687 Volunteers. Food and Drug Administration.

688 36. Liu C, Bayer A, Cosgrove SE, Daum RS, Fridkin SK, Gorwitz RJ, Kaplan SL, Karchmer AW,
689 Levine DP, Murray BE, J. Rybak M, Talan DA, Chambers HF. 2011. Clinical Practice
690 Guidelines by the Infectious Diseases Society of America for the Treatment of Methicillin-
691 Resistant *Staphylococcus aureus* Infections in Adults and Children: Executive Summary. Clin
692 Infect Dis 52:285–292.

693 37. Klockgether J, Cramer N, Wiehlmann L, Davenport CF, Tümmler B. 2011. *Pseudomonas*
694 *aeruginosa* Genomic Structure and Diversity. Front Microbiol 2.

695 38. Allen JP, Ozer EA, Minasov G, Shuvalova L, Kiryukhina O, Anderson WF, Satchell KJF, Hauser
696 AR. 2020. A comparative genomics approach identifies contact-dependent growth
697 inhibition as a virulence determinant. Proc Natl Acad Sci 117:6811–6821.

39. Iglewski BH. 1996. Pseudomonas, p. . *In* Baron, S (ed.), Medical Microbiology, 4th ed. University of Texas Medical Branch at Galveston, Galveston (TX).

40. Okuda J, Hayashi N, Okamoto M, Sawada S, Minagawa S, Yano Y, Gotoh N. 2010. Translocation of *Pseudomonas aeruginosa* from the intestinal tract is mediated by the binding of ExoS to an Na,K-ATPase regulator, FXYD3. Infect Immun 78:4511–4522.

41. Marshall JC, Christou NV, Meakins JL. 1993. The gastrointestinal tract. The "undrained abscess" of multiple organ failure. Ann Surg 218:111–119.

42. Abel S, Abel zur Wiesch P, Chang H-H, Davis BM, Lipsitch M, Waldor MK. 2015. Sequence tag-based analysis of microbial population dynamics. Nat Methods 12:223–226, 3 p following 226.

43. Hullahalli K, Pritchard JR, Waldor MK. Refined Quantification of Infection Bottlenecks and Pathogen Dissemination with STAMPR. mSystems 6:e00887-21.

44. Bachta KER, Allen JP, Cheung BH, Chiu C-H, Hauser AR. 2020. Systemic infection facilitates transmission of *Pseudomonas aeruginosa* in mice. 1. Nat Commun 11:543.

45. Cavalli-Sforza LL, Edwards AWF. 1967. Phylogenetic analysis. Models and estimation procedures. Am J Hum Genet 19:233–257.

46. Rosa CP, Pereira JA, Cristina de Melo Santos N, Brancaglion GA, Silva EN, Tagliati CA, Novaes RD, Corsetti PP, de Almeida LA. 2020. Vancomycin-induced gut dysbiosis during *Pseudomonas aeruginosa* pulmonary infection in a mice model. J Leukoc Biol 107:95–104.

717 47. Ray P, Pandey U, Aich P. 2021. Comparative analysis of beneficial effects of vancomycin
718 treatment on Th1- and Th2-biased mice and the role of gut microbiota. J Appl Microbiol
719 130:1337–1356.

720 48. Nazzal L, Soiefer L, Chang M, Tamizuddin F, Schatoff D, Cofer L, Aguero-Rosenfeld ME,
721 Matalon A, Meijers B, Holzman R, Lowenstein J. 2021. Effect of Vancomycin on the Gut
722 Microbiome and Plasma Concentrations of Gut-Derived Uremic Solutes. Kidney Int Rep
723 6:2122–2133.

724 49. Vrieze A, Out C, Fuentes S, Jonker L, Reuling I, Kootte RS, van Nood E, Holleman F, Knaapen
725 M, Romijn JA, Soeters MR, Blaak EE, Dallinga-Thie GM, Reijnders D, Ackermans MT, Serlie
726 MJ, Knop FK, Holst JJ, van der Ley C, Kema IP, Zoetendal EG, de Vos WM, Hoekstra JBL,
727 Stroes ES, Groen AK, Nieuwdorp M. 2014. Impact of oral vancomycin on gut microbiota,
728 bile acid metabolism, and insulin sensitivity. J Hepatol 60:824–831.

729 50. Kim E, Kim AH, Lee Y, Ji SC, Cho J-Y, Yu K-S, Chung J-Y. 2021. Effects of vancomycin-induced
730 gut microbiome alteration on the pharmacodynamics of metformin in healthy male
731 subjects. Clin Transl Sci 14:1955–1966.

732 51. Calderon-Gonzalez R, Lee A, Lopez-Campos G, Hancock SJ, Sa-Pessoa J, Dumigan A,
733 McMullan R, Campbell EL, Bengoechea JA. 2023. Modelling the Gastrointestinal Carriage of
734 *Klebsiella pneumoniae* Infections. mBio 14:e03121-22.

735 52. Cheung BH, Alisoltani A, Kochan TJ, Lebrun-Corbin M, Nozick SH, Axline CMR, Bachta KER,
736 Ozer EA, Hauser AR. 2023. Genome-wide screens reveal shared and strain-specific genes
737 that facilitate enteric colonization by *Klebsiella pneumoniae*. mBio 14:e0212823.

738 53. Westerman TL, McClelland M, Elfenbein JR. 2021. YeiE Regulates Motility and Gut
739 Colonization in *Salmonella enterica* Serotype Typhimurium. mBio 12:10.1128/mbio.03680-
740 20.

741 54. Krypotou E, Townsend GE, Gao X, Tachiyama S, Liu J, Pokorzynski ND, Goodman AL,
742 Groisman EA. 2023. Bacteria require phase separation for fitness in the mammalian gut.
743 Science 379:1149–1156.

744 55. Merrell DS, Hava DL, Camilli A. 2002. Identification of novel factors involved in colonization
745 and acid tolerance of *Vibrio cholerae*. Mol Microbiol 43:1471–1491.

746 56. Smith EE, Buckley DG, Wu Z, Saenphimmachak C, Hoffman LR, D'Argenio DA, Miller SI,
747 Ramsey BW, Speert DP, Moskowitz SM, Burns JL, Kaul R, Olson MV. 2006. Genetic
748 adaptation by *Pseudomonas aeruginosa* to the airways of cystic fibrosis patients. Proc Natl
749 Acad Sci 103:8487–8492.

750 57. Mena A, Smith EE, Burns JL, Speert DP, Moskowitz SM, Perez JL, Oliver A. 2008. Genetic
751 Adaptation of *Pseudomonas aeruginosa* to the Airways of Cystic Fibrosis Patients Is
752 Catalyzed by Hypermutation. J Bacteriol 190:7910–7917.

753 58. Eklöf J, Misiakou MA, Sivapalan P, Armbruster K, Browatzki A, Nielsen TL, Lapperre TS,
754 Andreassen HF, Janner J, Ulrik CS, Gabrielaite M, Johansen HK, Jensen A, Nielsen TV, Hertz

FB, Ghathian K, Calum H, Wilcke T, Seersholm N, Jensen J-US, Marvig RL. 2022. Persistence and genetic adaptation of *Pseudomonas aeruginosa* in patients with chronic obstructive pulmonary disease. Clin Microbiol Infect 28:990–995.

59. Chancharoenthana W, Kamolratanakul S, Schultz MJ, Leelahavanichkul A. 2023. The leaky gut and the gut microbiome in sepsis – targets in research and treatment. Clin Sci Lond Engl 1979 137:645–662.

60. Hullahalli K, Waldor MK. 2021. Pathogen clonal expansion underlies multiorgan dissemination and organ-specific outcomes during murine systemic infection. eLife 10:e70910.

61. Louie A, Zhang T, Becattini S, Waldor MK, Portnoy DA. 2019. A Multiorgan Trafficking Circuit Provides Purifying Selection of *Listeria monocytogenes* Virulence Genes. mBio 10:10.1128/mbio.02948-19.

62. Campbell IW, Hullahalli K, Turner JR, Waldor MK. 2023. Quantitative dose-response analysis untangles host bottlenecks to enteric infection. Nat Commun 14:456.

63. Sun Y, Koyama Y, Shimada S. 2022. Measurement of intraluminal pH changes in the gastrointestinal tract of mice with gastrointestinal diseases. Biochem Biophys Res Commun 620:129–134.

64. Tsuji A, Kaneko Y, Takahashi K, Ogawa M, Goto S. 1982. The Effects of Temperature and pH on the Growth of Eight Enteric and Nine Glucose Non-Fermenting Species of Gram-Negative Rods. Microbiol Immunol 26:15–24.

775 65. Scheetz MH, Hoffman M, Bolon MK, Schulert G, Estrellado W, Baraboutis IG, Sriram P, Dinh
776 M, Owens LK, Hauser AR. 2009. Morbidity Associated with *Pseudomonas aeruginosa*
777 Bloodstream Infections. Diagn Microbiol Infect Dis 64:311–319.

778 66. Vogel HJ, Bonner DM. 1956. Acetylornithinase of *Escherichia coli*: partial purification and
779 some properties. J Biol Chem 218:97–106.

780

781 **Figure Legends**
782
783 **Figure 1: Murine model of *P. aeruginosa* GI carriage**. (A) PABL048 fecal burden after
784 an orogastric gavage with $10^{5.6}$ CFU. Male (square) or female (circle) mice received
785 either PBS (gray symbols) or vancomycin (colored symbols) injections, and an
786 orogastric gavage with $10^{5.6}$ CFU of PABL048. The experiment was performed twice for
787 vancomycin treated mice (combined results are shown; n ≥ 8), and once for PBS
788 treated mice (n = 5). Each symbol represents one mouse. Solid horizontal lines indicate
789 medians. No significant differences in fecal CFU were found at any time point between
790 male and female mice (multiple t-tests). (B) Timeline schematic of the model. Mice were
791 intraperitoneally injected daily with vancomycin for 7 days at a dose of 370 mg/kg. On
792 the fifth day of vancomycin treatment (day 0), mice received a defined dose of *P.*
793 *aeruginosa* through orogastric gavage. On selected days, feces were collected to
794 assess the extent of GI carriage, estimated by CFU counts. (C) Fecal burden of six
795 clinical isolates of *P. aeruginosa* during GI carriage. Vancomycin and bacterial delivery
796 (inoculum sizes: $10^{5.4+/-0.2}$ CFU PABL004, $10^{5.6+/-0.3}$ CFU PABL006, $10^{6+/-0.2}$ CFU
797 PABL012, $10^{5.4+/-0.1}$ CFU PABL048, $10^{6+/-0.1}$ PABL049 or $10^{6+/-0.1}$ CFU PABL054) were
798 performed as in B. Box plots are shown with boxes extending from the 25th to 75th
799 percentiles, whiskers representing minimum and maximum values and lines indicating
800 medians. Experiments were performed at least twice, and combined results are shown
801 (n ≥ 10). *p ≤ 0.05, **p ≤ 0.01 (t-tests with Holm-Sidak correction for multiple
802 comparisons). The dotted line indicates the limit of detection.
803
804 **Figure 2: Tissue histology of the GI tracts of mice with carriage of *P. aeruginosa***.
805 Hematoxylin-eosin staining of organ tissues collected at day 3 post-inoculation with
806 either $10^{7.1}$ CFU of PABL048 or PBS (Mock). Prior to the orogastric gavage, mice
807 received either vancomycin or PBS through intraperitoneal injections. Images in the
808 bottom 4 rows were captured at a 400x magnification (bar = 100 μm). Images on the top
809 row were captured at a 1,000x magnification (bar = 200 μm). (n = 3-4 mice/group).
810 Arrows indicate intraluminal clumps of bacterial bacilli.
811

Figure 3: Dissemination of *P. aeruginosa* from the GI tract. *P. aeruginosa* burden in organs of mice carrying PABL048. Mice were sacrificed at (A) day 3 (n = 10), (B) day 7 (n = 10) or (C) day 14 (n = 9) post-orogastric gavage with $10^{7.4+/-0.2}$ CFU of PABL048, and bacterial CFU in the organs were enumerated by plating. The experiment was performed twice; combined results are shown. Each symbol represents one mouse. Solid horizontal lines indicate medians. The vertical dashed lines separate GI tract organs (left) from other organs (right). Symbols representing mice with dissemination from the GI tract are colored (one color/mouse). The horizontal dotted line indicates the limit of detection.

Figure 4: Long-term carriage of *P. aeruginosa* in the GI tract. PABL048 fecal burdens after an orogastric gavage with $10^{5.7+/-0.3}$ CFU in male (purple squares) and female (red circles) mice. The experiment was performed twice; combined results are shown (n = 10). Each symbol represents one mouse. Solid horizontal lines indicate medians. No significant differences were found between male and female mice at any time point (multiple t-tests). The dotted line indicates the limit of detection.

Figure 5: Founding populations and bacterial loads of *P. aeruginosa* in the GI tract. A total of $10^{6.1}$ CFU of $PABL012_{pool}$ were delivered to single-caged mice by orogastric gavage. *P. aeruginosa* CFU in 250 µL of resuspensions of collected homogenized tissues (one-fourth of tissue homogenates of stomach, small intestine ["s. intestine"], caecum, colon, and feces) were enumerated by plating, and founding population sizes (N_s) were estimated using the STAMPR approach. (A-C) Bacterial loads (CFU, black circles) and estimated founding population sizes (N_s, pink circles) were quantified at (A) 24 (n = 5), (B) 48 (n = 4) and (C) 72 hpi (n = 3, except for N_s in stomach, which was n = 2 due to a sequencing issue). Each circle represents an organ from one mouse. Solid horizontal lines indicate medians. Minor ticks on the right Y axis represent the limits of detection for the CFU. Triangles represent samples with no recovered CFU. (D) *P. aeruginosa* burdens and (E) estimated founding population sizes in different tissues of the GI tract at 24 (purple), 48 (blue) and 72 (green) hpi. For comparison, fecal samples were collected at 24 hpi ("feces 24 hpi") regardless of the ending timepoint. An additional terminal fecal sample was available for animals harvested at 48 or 72 hpi ("feces late"). Squares represent medians, and error bars represent 95% confidence intervals. The dotted line indicates the limit of detection for CFU. N_s values are not significantly different over time (t-test).

Figure 6: Average intra-mouse genetic relatedness of *P. aeruginosa* populations in the GI tract. (A-C) Heatmaps representing the average intra-mouse genetic distances (GDs) of *P. aeruginosa* from organs of the mice described in figure 5, at (A) 24, (B) 48, and (C) 72 hpi. Lower values of GD (purple) indicate a higher frequency of barcode sharing between the samples, with 0 reflecting identical populations. (D) GD values over time between: stomach and small intestine ("SI") (green), small intestine and caecum (teal), and caecum and colon (purple). Each symbol represents one mouse. Lines indicate medians. (E-G) Heatmaps representing the average intra-mouse Fractional Resilient Genetic Distances (FRD) of *P. aeruginosa* from organs of the mice described in figure 5, at (E) 24, (F) 48 and (G) 72 hpi. The FRD is calculated using the

following formula: $FRD_{A-B} = \frac{\ln(RD_{A-B}+1)}{\ln(Number\ of\ barcodes\ in\ B+1)}$ where $RD_{A\text{-}B}$ is the number of shared barcodes that contribute to genetic similarity between samples A and B. The column names in the FRD heatmaps correspond to the organ of reference (B in the above formula). High FRD values (yellow) indicate that most bacterial barcodes are shared between samples. Thick lines in panels B-C, F-G separate the samples collected at the time of dissection (top/left) from samples of feces collected from the same animals at an earlier time point ("feces 24h") (bottom/right). Samples outlined by blue and orange squares in panels A and E indicate pairs that are detailed in panel H. (H) FRD values for bacteria from the stomach/small intestine (SI) (blue) and small intestine/caecum (orange) pairs at 24 hpi. Each symbol represents one mouse. Lines indicate medians. p-values are indicated (two-tailed paired t test). The Venn diagrams under the graph are visual representations of the averaged proportion of barcodes shared between two adjacent organs (circles). Diagrams created using Biorender.com. As observed in figure 5, no bacteria could be detected in the stomach of some mice, leading to variation in the number of samples used for this analysis: A, E, H: n = 5 (except for the stomach; n = 4), B, F: n = 4 (except for the stomach; n = 3), C, G: n = 3 (except for the stomach; n = 1), D: see panels A-C.

Figure 7: Model of the population dynamics of *P. aeruginosa* following orogastric gavage. Left: soon after the orogastric delivery of *P. aeruginosa*, most bacteria are eliminated from the stomach, severely constricting the size of the remaining population (less than 0.01% survival). Part of the population passes through the stomach to reach other compartments of the GI tract: small intestine, caecum, colon, and feces. *P. aeruginosa* does not encounter additional barriers downstream from the stomach. Right: over the first 24 hours, population expansion and/or reflux from the small intestine occurs in the stomach. The small intestine and the caecum support massive expansion of the remaining *P. aeruginosa* clones, and bacteria freely migrate from the caecum to the colon and feces. This figure was created using Biorender.com.

Supplemental Figure Legends

Supplemental Figure 1: GI carriage of *P. aeruginosa* obtained with various regimens of vancomycin treatment. Mice received daily injections of vancomycin for various times before and after orogastric gavage ("x + y days" with x = the number of days of vancomycin injections prior to and on the day of orogastric gavage, and y = the number of days of vancomycin injections after the bacterial inoculation). Orogastric gavage was performed with $10^{5.8+/-0.2}$ CFU of strain PABL048. Each symbol represents one mouse.
Solid horizontal lines indicate medians. The experiment was performed twice (combined results shown; n = 10)). The dotted line indicates the limit of detection. *p ≤ 0.05, **p ≤ 0.01 (t-tests). Significant differences were not detected for any of the time points between mice treated with 5 + 2 days and 3+ 2 days of vancomycin.

Supplemental Figure 2: Fecal burden of strain PABL048 at day 3 post-inoculation. Mice were treated with either PBS (pink) or vancomycin (black and teal) for 7 days. On the fifth day of treatment, mice received either PBS (black) or $10^{7.1}$ CFU of PABL048 through orogastric gavage (pink and teal). The experiment was performed once (n=3-4 animals/group). Each symbol represents one mouse. Lines indicate medians. The dotted line indicates the limit of detection.

Supplemental Figure 3: Recovery of *P. aeruginosa* from the GI tract at early times following inoculation. *P. aeruginosa* burden in GI tissues of mice gavaged with PABL012. Mice were sacrificed at (A) 1 h (n = 5) or (B) 6 h (n = 5) post-orogastric gavage with $10^{6.1}$ CFU of PABL012, and bacterial CFU in the organs were enumerated by plating. Experiment performed once. Red circles represent the inoculums. Each black circle represents one mouse. Solid horizontal lines indicate medians. The horizontal dotted line indicates the limit of detection. Open circles represent tissues with CFU bellow the limit of detection.

Supplemental Figure 4: Ratio of bacterial recovery vs. founding population in GI sites. Tissues were harvested at 24 (purple, n = 5), 48 (blue, n = 4) or 72 hours (green, n = 3) after orogastric gavage with $PABL012_{pool}$. Fecal samples were collected at 24 hpi ("feces 24 hpi") regardless of the ending timepoint. Additional terminal fecal sample timepoints were available for animals that had organs harvested at 48 or 72 hpi ("feces late"). CFU/N_s ratios were calculated. Squares represent medians, and error bars represent the 95% confidence intervals.

Supplemental Figure 5: Barcode frequency distributions of *P. aeruginosa* bacteria recovered from mice following orogastric inoculation. The frequencies of unique barcodes in each bacterial population from different sites are shown. (A) Inoculum samples. Barcode frequency was analyzed in the 26 bacterial aliquots that were each used to inoculate a different mouse in the STAMP experiment. Six representative frequency distributions are shown. (B-D) Barcode frequency distributions after noise removal for the output samples from mice sacrificed at (B) 24, (C) 48 or (D) 72 hours post-orogastric gavage. Each dot represents the frequency at which one specific

935 barcode was detected. For each mouse ("M#"), dots representing the most frequent
936 clones identified in the stomach are colored blue in all organs, and dots representing the
937 most frequent clones identified in the small intestine are colored red.
938

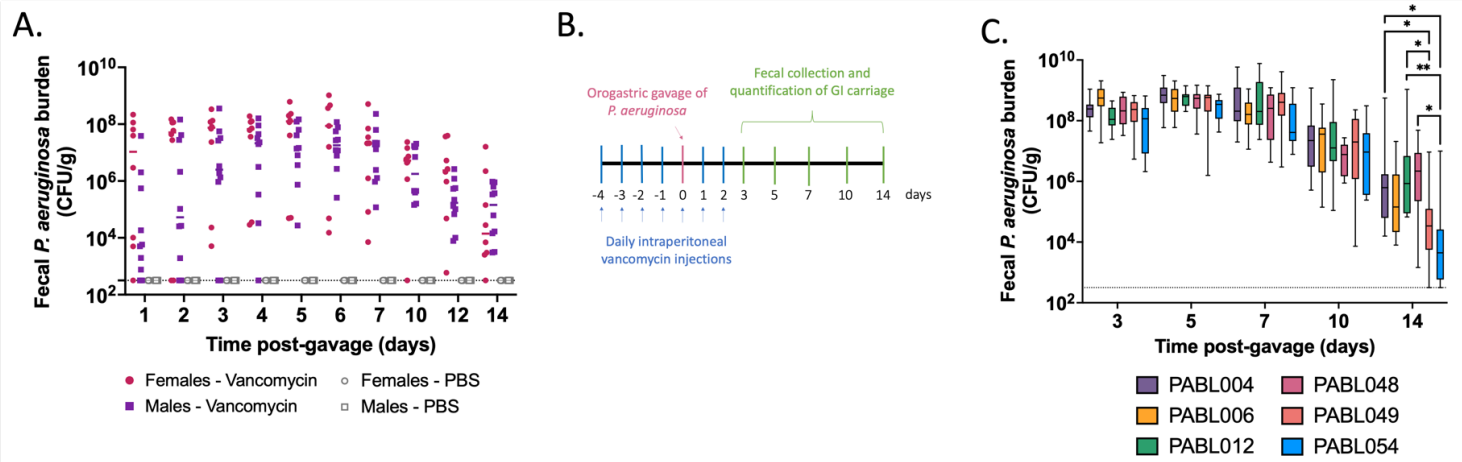

Figure 1: Murine model of *P. aeruginosa* GI carriage. (A) PABL048 fecal burden after an orogastric gavage with $10^{5.6}$ CFU. Male (square) or female (circle) mice received either PBS (gray symbols) or vancomycin (colored symbols) injections, and an orogastric gavage with $10^{5.6}$ CFU of PABL048. The experiment was performed twice for vancomycin treated mice (combined results are shown; n ≥ 8), and once for PBS treated mice (n = 5). Each symbol represents one mouse. Solid horizontal lines indicate medians. No significant differences in fecal CFU were found at any time point between male and female mice (multiple t-tests). (B) Timeline schematic of the model. Mice were intraperitoneally injected daily with vancomycin for 7 days at a dose of 370 mg/kg. On the fifth day of vancomycin treatment (day 0), mice received a defined dose of *P. aeruginosa* through orogastric gavage. On selected days, feces were collected to assess the extent of GI carriage, estimated by CFU counts. (C) Fecal burden of six clinical isolates of *P. aeruginosa* during GI carriage. Vancomycin and bacterial delivery (inoculum sizes: $10^{5.4+/-0.2}$ CFU PABL004, $10^{5.6+/-0.3}$ CFU PABL006, $10^{6+/-0.2}$ CFU PABL012, $10^{5.4+/-0.1}$ CFU PABL048, $10^{6+/-0.1}$ PABL049 or $10^{6+/-0.1}$ CFU PABL054) were performed as in B. Box plots are shown with boxes extending from the 25th to 75th percentiles, whiskers representing minimum and maximum values and lines indicating medians. Experiments were performed at least twice, and combined results are shown (n ≥ 10). *p ≤ 0.05, **p ≤ 0.01 (t-tests with Holm-Sidak correction for multiple comparisons). The dotted line indicates the limit of detection.

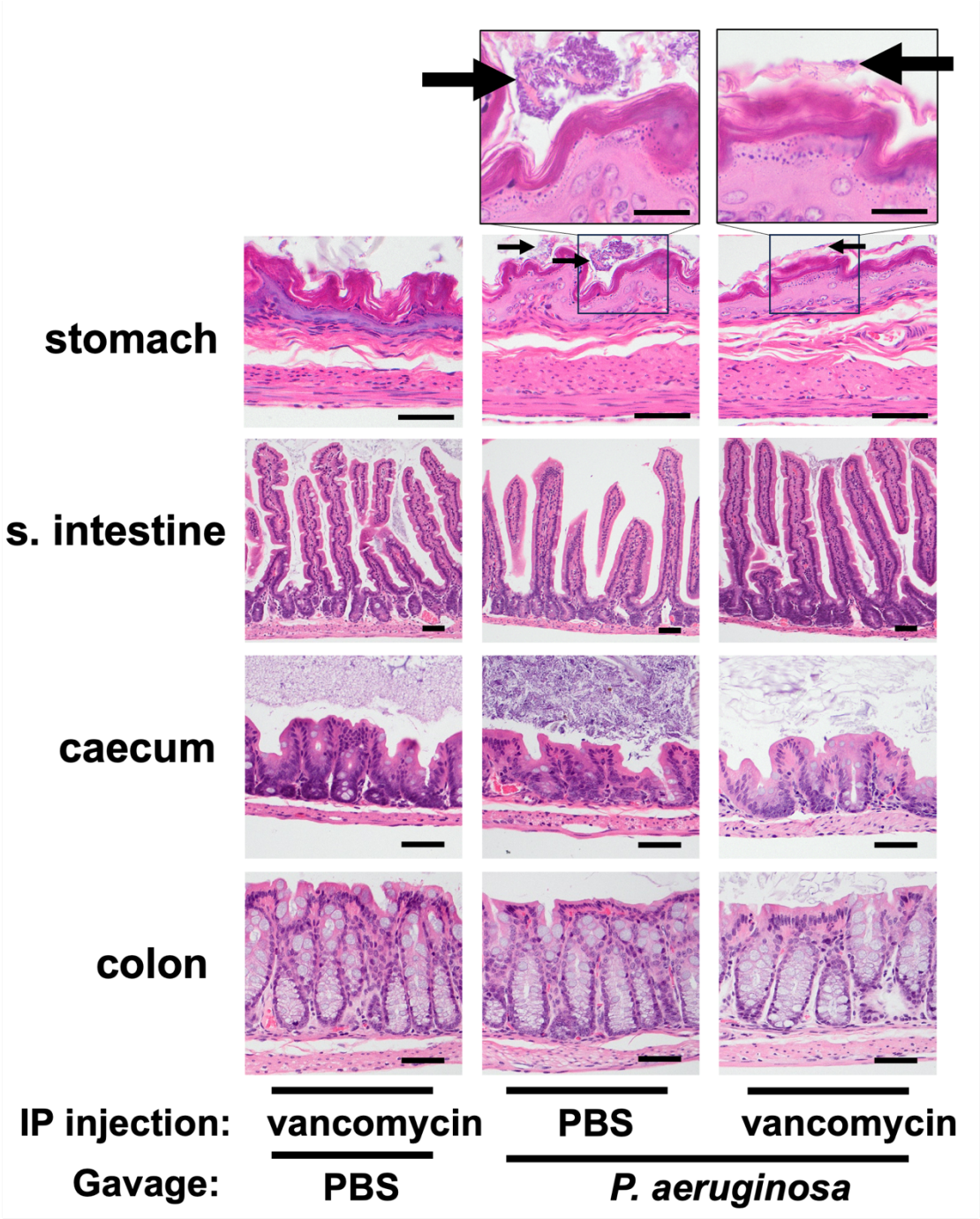

Figure 2: Tissue histology of the GI tracts of mice with carriage of *P. aeruginosa*. Hematoxylin-eosin staining of organ tissues collected at day 3 post-inoculation with either $10^{7.1}$ CFU of PABL048 or PBS (Mock). Prior to the orogastric gavage, mice received either vancomycin or PBS through intraperitoneal injections. Images in the bottom 4 rows were captured at a 400x magnification (bar = 100 μm). Images on the top row were captured at a 1,000x magnification (bar = 200 μm). (n = 3-4 mice/group). Arrows indicate intraluminal clumps of bacterial bacilli.

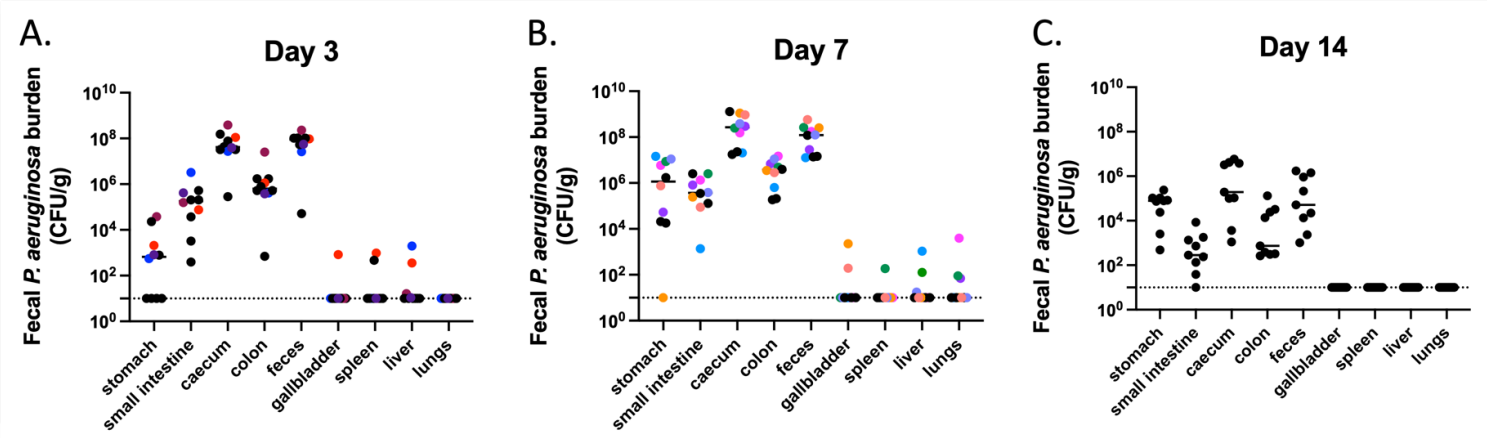

Figure 3: Dissemination of *P. aeruginosa* from the GI tract. *P. aeruginosa* burden in organs of mice carrying PABL048. Mice were sacrificed at (A) day 3 (n = 10), (B) day 7 (n = 10) or (C) day 14 (n = 9) post-orogastric gavage with $10^{7.4+/-0.2}$ CFU of PABL048, and bacterial CFU in the organs were enumerated by plating. The experiment was performed twice; combined results are shown. Each symbol represents one mouse. Solid horizontal lines indicate medians. The vertical dashed lines separate GI tract organs (left) from other organs (right). Symbols representing mice with dissemination from the GI tract are colored (one color/mouse). The horizontal dotted line indicates the limit of detection.

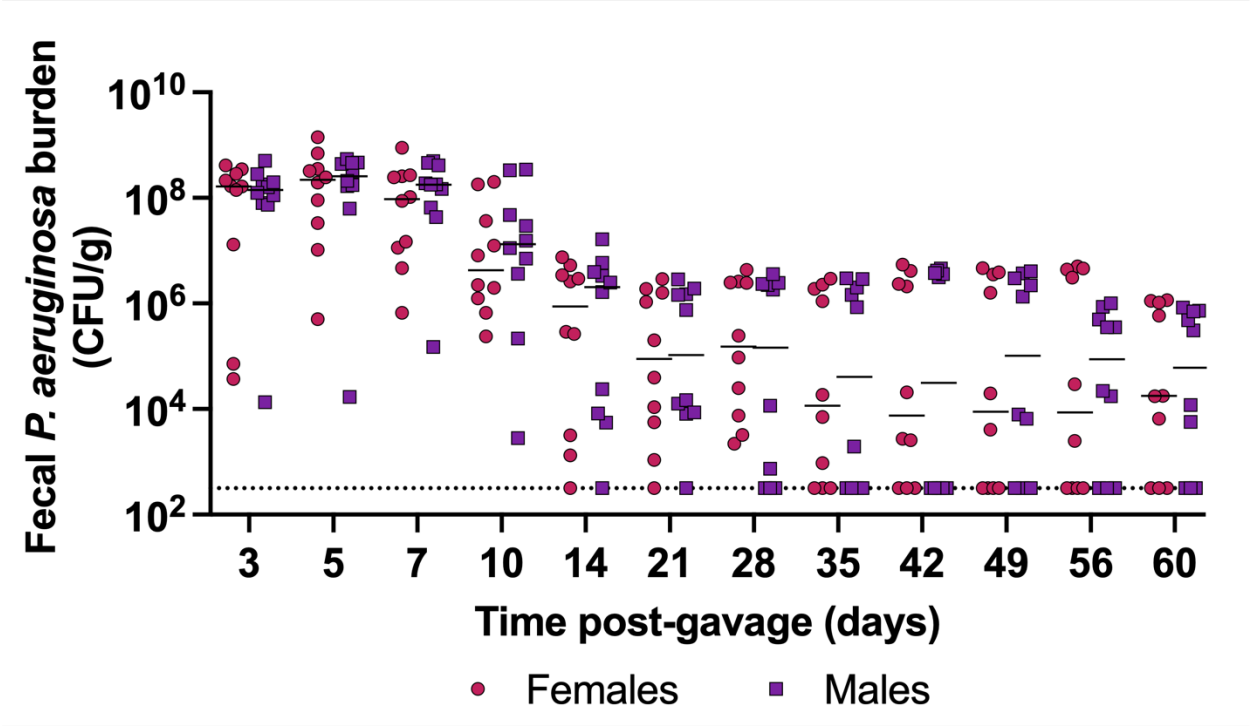

Figure 4: Long-term carriage of *P. aeruginosa* in the GI tract. PABL048 fecal burdens after an orogastric gavage with $10^{5.7+/-0.3}$ CFU in male (purple squares) and female (red circles) mice. The experiment was performed twice; combined results are shown (n = 10). Each symbol represents one mouse. Solid horizontal lines indicate medians. No significant differences were found between male and female mice at any time point (multiple t-tests). The dotted line indicates the limit of detection.

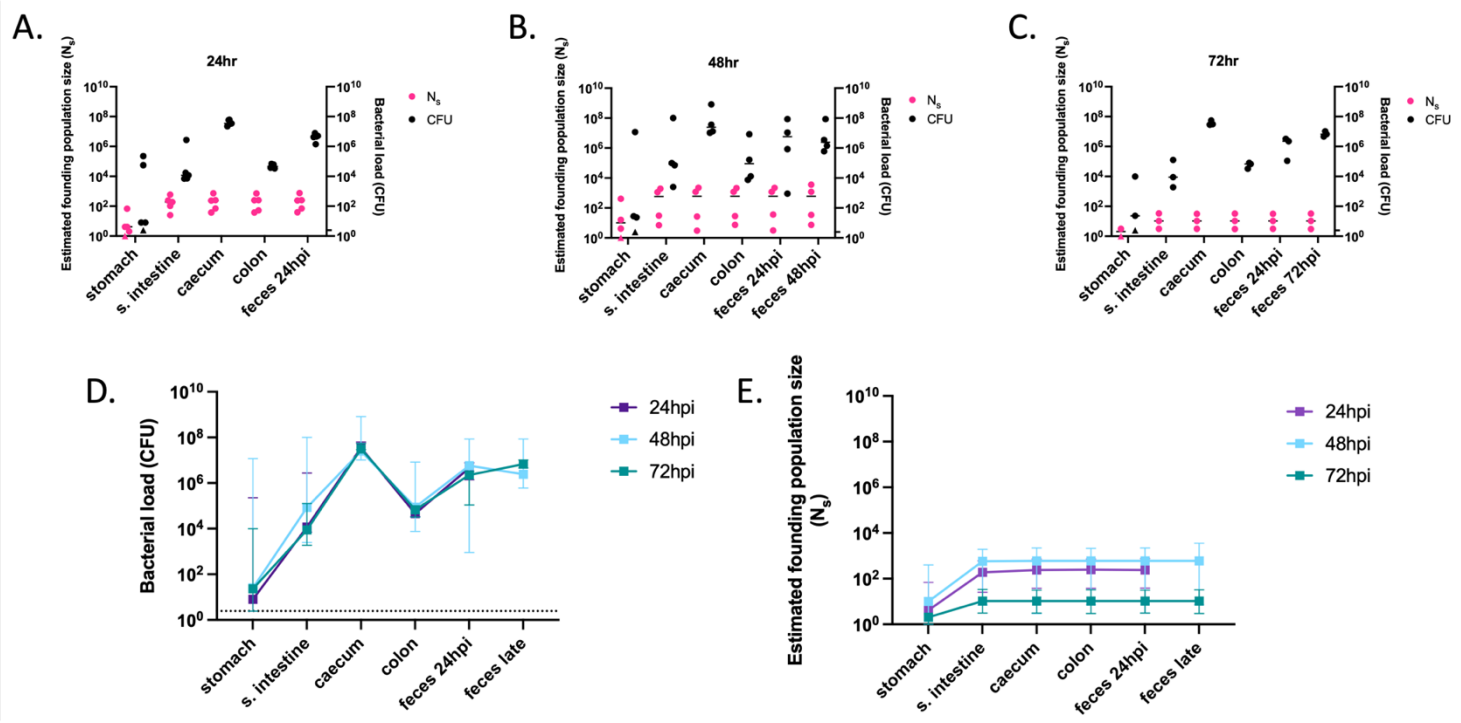

Figure 5: Founding populations and bacterial loads of *P. aeruginosa* in the GI tract. A total of $10^{6.1}$ CFU of $PABL012_{pool}$ were delivered to single-caged mice by orogastric gavage. *P. aeruginosa* CFU in 250 µL of resuspensions of collected homogenized tissues (one-fourth of tissue homogenates of stomach, small intestine ["s. intestine"], caecum, colon, and feces) were enumerated by plating, and founding population sizes (N_s) were estimated using the STAMPR approach. (A-C) Bacterial loads (CFU, black circles) and estimated founding population sizes (N_s, pink circles) were quantified at (A) 24 (n = 5), (B) 48 (n = 4) and (C) 72 hpi (n = 3, except for N_s in stomach, which was n = 2 due to a sequencing issue). Each circle represents an organ from one mouse. Solid horizontal lines indicate medians. Minor ticks on the right Y axis represent the limits of detection for the CFU. Triangles represent samples with no recovered CFU. (D) *P. aeruginosa* burdens and (E) estimated founding population sizes in different tissues of the GI tract at 24 (purple), 48 (blue) and 72 (green) hpi. For comparison, fecal samples were collected at 24 hpi ("feces 24 hpi") regardless of the ending timepoint. An additional terminal fecal sample was available for animals harvested at 48 or 72 hpi ("feces late"). Squares represent medians, and error bars represent 95% confidence intervals. The dotted line indicates the limit of detection for CFU. N_s values are not significantly different over time (t-test).

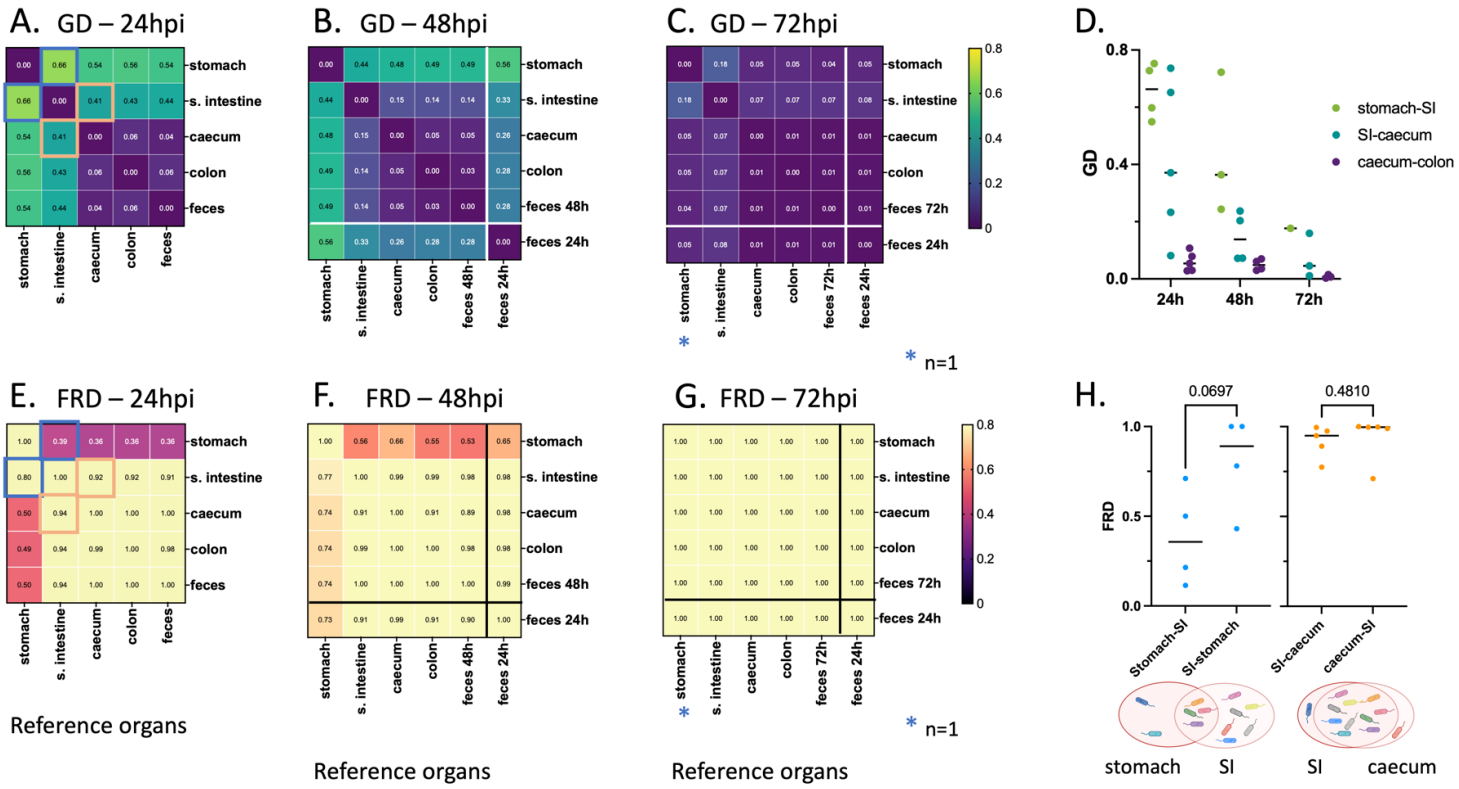

Figure 6: Average intra-mouse genetic relatedness of *P. aeruginosa* populations in the GI tract. (A-C) Heatmaps representing the average intra-mouse genetic distances (GDs) of *P. aeruginosa* from organs of the mice described in figure 5, at (A) 24, (B) 48, and (C) 72 hpi. Lower values of GD (purple) indicate a higher frequency of barcode sharing between the samples, with 0 reflecting identical populations. (D) GD values over time between: stomach and small intestine ("SI") (green), small intestine and caecum (teal), and caecum and colon (purple). Each symbol represents one mouse. Lines indicate medians. (E-G) Heatmaps representing the average intra-mouse Fractional Resilient Genetic Distances (FRD) of *P. aeruginosa* from organs of the mice described in figure 5, at (E) 24, (F) 48 and (G) 72 hpi. The FRD is calculated using the following formula: $FRD_{A-B} = \frac{\ln(RD_{A-B}+1)}{\ln(Number\ of\ barcodes\ in\ B+1)}$ where $RD_{A\text{-}B}$ is the number of shared barcodes that contribute to genetic similarity between samples A and B. The column names in the FRD heatmaps correspond to the organ of reference (B in the above formula). High FRD values (yellow) indicate that most bacterial barcodes are shared between samples. Thick lines in panels B-C, F-G separate the samples collected at the time of dissection (top/left) from samples of feces collected from the same animals at an earlier time point ("feces 24h") (bottom/right). Samples outlined by blue and orange squares in panels A and E indicate pairs that are detailed in panel H. (H) FRD values for bacteria from the stomach/small intestine (SI) (blue) and small intestine/caecum (orange) pairs at 24 hpi. Each symbol represents one mouse. Lines indicate medians. p-values are indicated (two-tailed paired t test). The Venn diagrams under the graph are visual representations of the averaged proportion of barcodes shared between two adjacent organs (circles). Diagrams created using Biorender.com. As observed in figure 5, no bacteria could be detected in the stomach of some mice, leading to variation in the number of samples used for this analysis: A, E, H: n = 5 (except for the stomach; n = 4), B, F: n = 4 (except for the stomach; n = 3), C, G: n = 3 (except for the stomach; n = 1), D: see panels A-C.

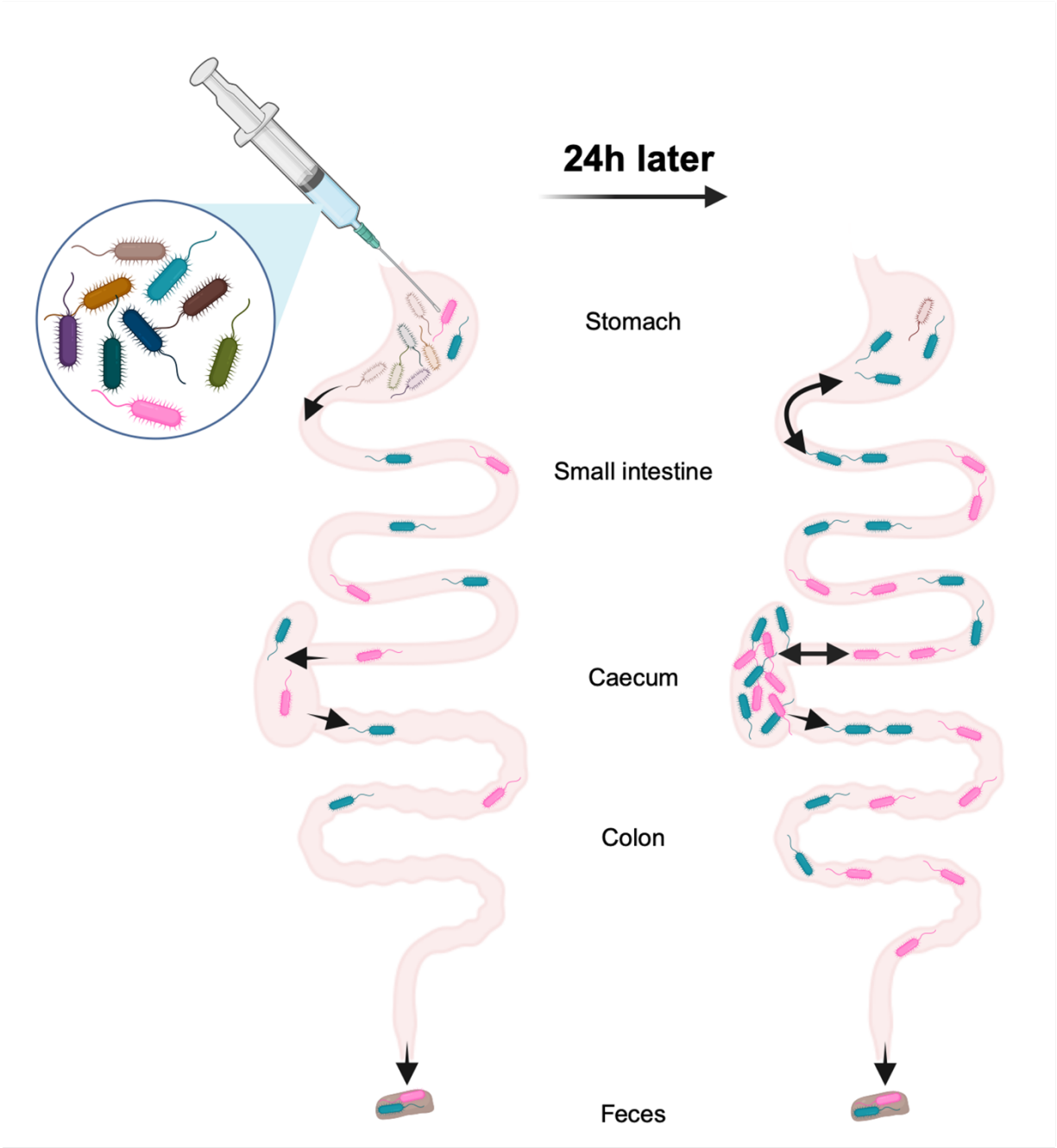

Figure 7: Model of the population dynamics of *P. aeruginosa* following orogastric gavage. Left: soon after the orogastric delivery of *P. aeruginosa*, most bacteria are eliminated from the stomach, severely constricting the size of the remaining population (less than 0.01% survival). Part of the population passes through the stomach to reach other compartments of the GI tract: small intestine, caecum, colon, and feces. *P. aeruginosa* does not encounter additional barriers downstream from the stomach. Right: over the first 24 hours, population expansion and/or reflux from the small intestine occurs in the stomach. The small intestine and the caecum support massive expansion of the remaining *P. aeruginosa* clones, and bacteria freely migrate from the caecum to the colon and feces. This figure was created using Biorender.com.

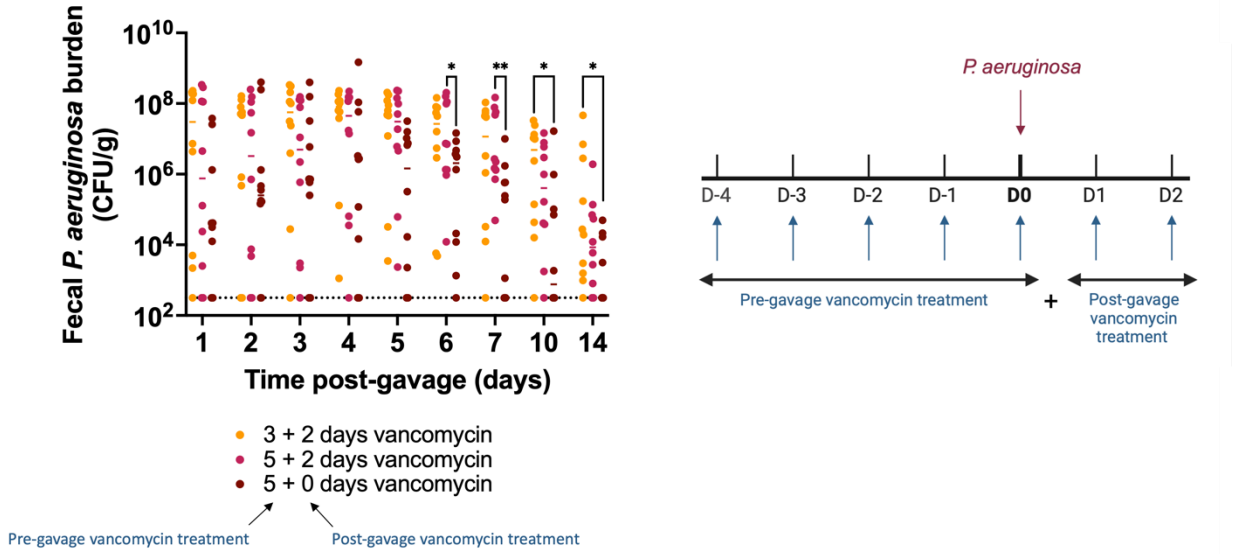

Supplemental Figure 1: GI carriage of *P. aeruginosa* obtained with various regimens of vancomycin treatment. Mice received daily injections of vancomycin for various times before and after orogastric gavage ("x + y days" with x = the number of days of vancomycin injections prior to and on the day of orogastric gavage, and y = the number of days of vancomycin injections after the bacterial inoculation). Orogastric gavage was performed with $10^{5.8+/-0.2}$ CFU of strain PABL048. Each symbol represents one mouse. Solid horizontal lines indicate medians. The experiment was performed twice (combined results shown; n = 10)). The dotted line indicates the limit of detection. *p ≤ 0.05, **p ≤ 0.01 (t-tests). Significant differences were not detected for any of the time points between mice treated with 5 + 2 days and 3+ 2 days of vancomycin.

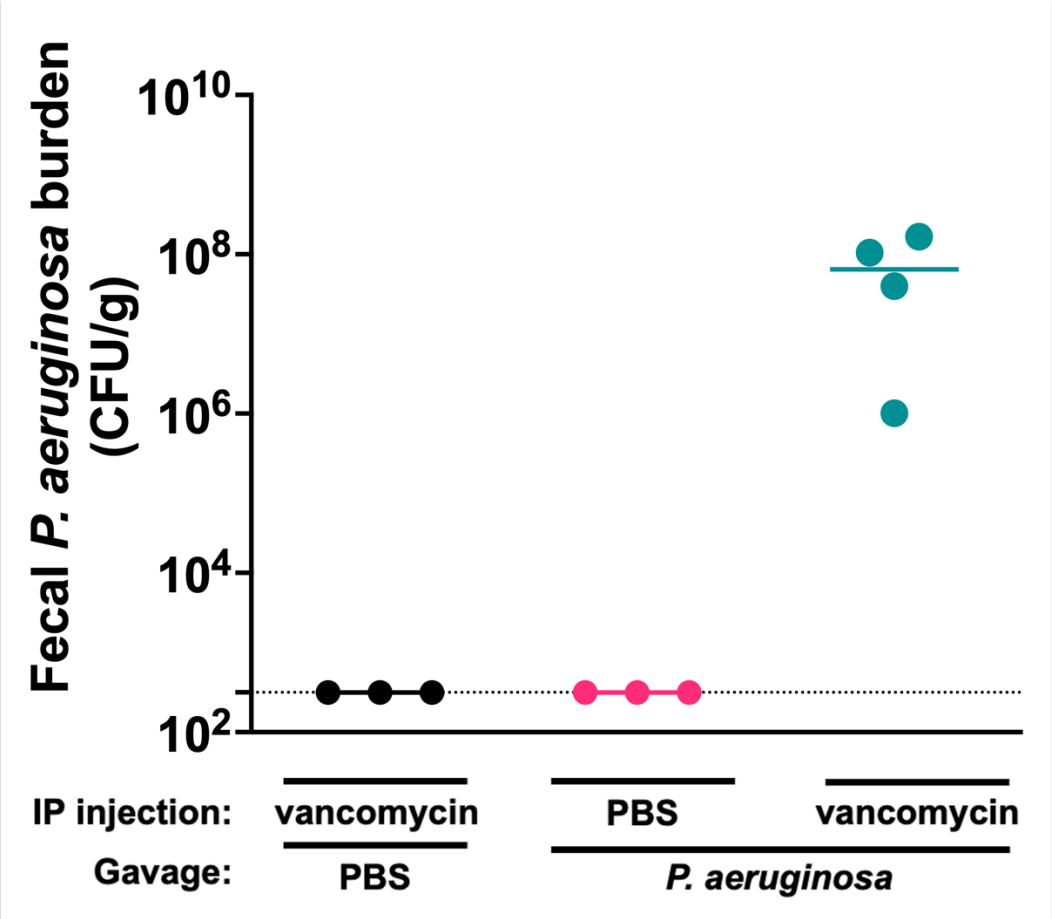

Supplemental Figure 2: Fecal burden of strain PABL048 at day 3 post-inoculation. Mice were treated with either PBS (pink) or vancomycin (black and teal) for 7 days. On the fifth day of treatment, mice received either PBS (black) or $10^{7.1}$ CFU of PABL048 through orogastric gavage (pink and teal). The experiment was performed once (n=3-4 animals/group). Each symbol represents one mouse. Lines indicate medians. The dotted line indicates the limit of detection.

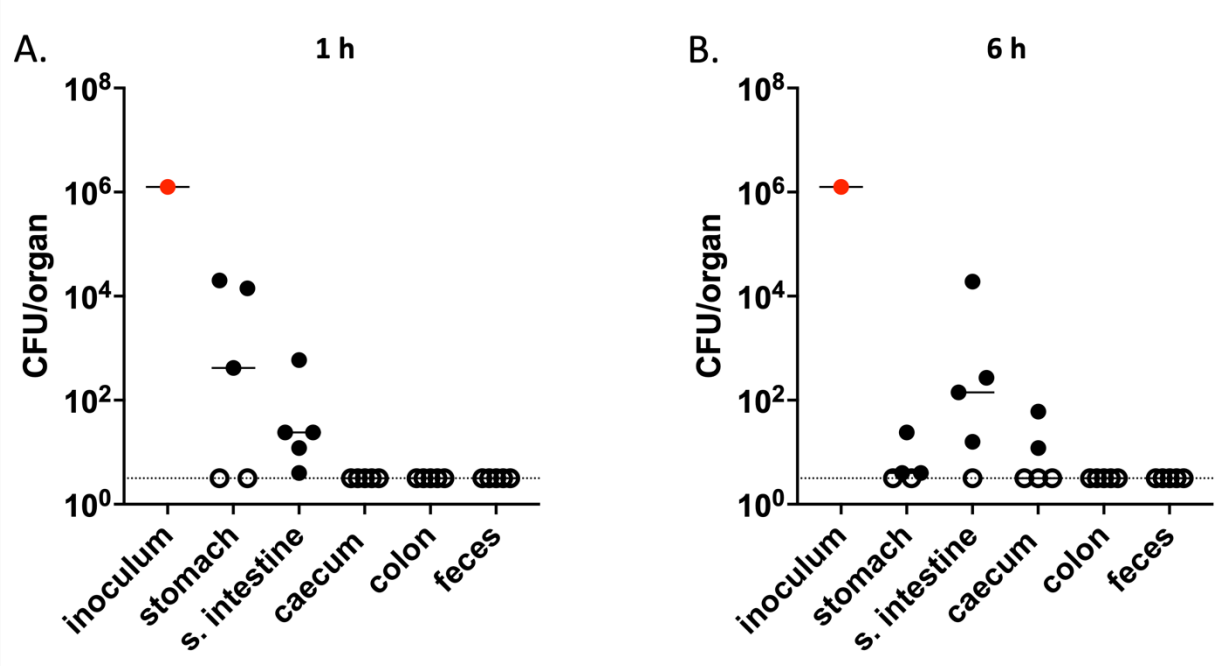

Supplemental Figure 3: Recovery of *P. aeruginosa* from the GI tract at early times following inoculation. *P. aeruginosa* burden in GI tissues of mice gavaged with PABL012. Mice were sacrificed at (A) 1 h (n = 5) or (B) 6 h (n = 5) post-orogastric gavage with $10^{6.1}$ CFU of PABL012, and bacterial CFU in the organs were enumerated by plating. Experiment performed twice with similar results but different limits of detection; figure shows one repeat. Red circles represent the inoculums. Each black circle represents one mouse. Solid horizontal lines indicate medians. The horizontal dotted line indicates the limit of detection. Open circles represent tissues with CFU bellow the limit of detection.

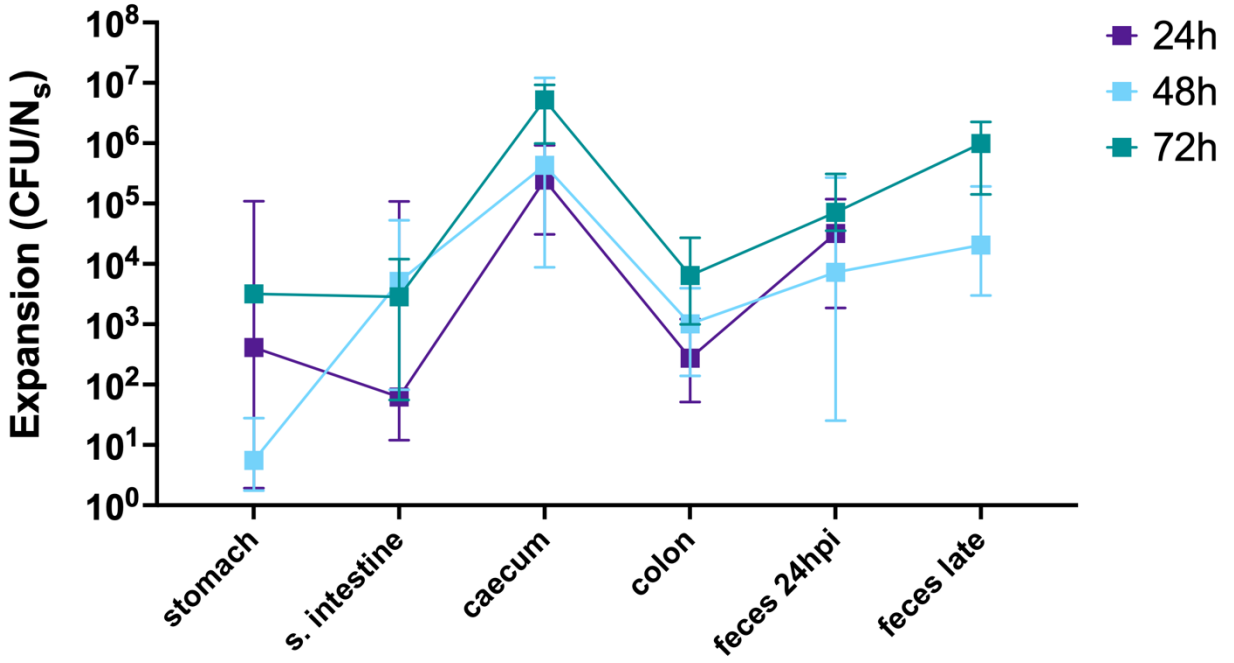

Supplemental Figure 4: Ratio of bacterial recovery vs. founding population in GI sites. Tissues were harvested at 24 (purple, n = 5), 48 (blue, n = 4) or 72 hours (green, n = 3) after orogastric gavage with $PABL012_{pool}$. Fecal samples were collected at 24 hpi ("feces 24 hpi") regardless of the ending timepoint. Additional terminal fecal sample timepoints were available for animals that had organs harvested at 48 or 72 hpi ("feces late"). CFU/N_s ratios were calculated. Squares represent medians, and error bars represent the 95% confidence intervals.

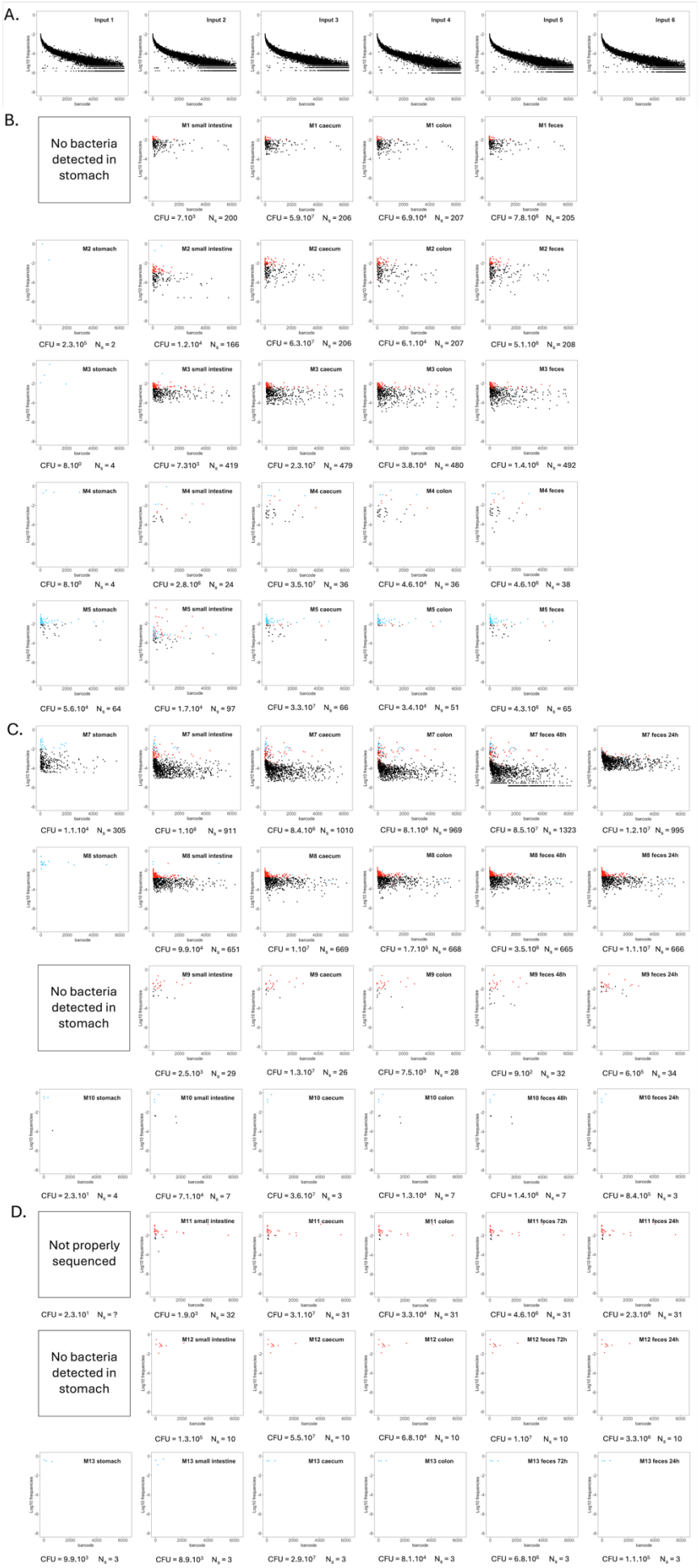

Supplemental Figure 5: Barcode frequency distributions of *P. aeruginosa* bacteria recovered from mice following orogastric inoculation. The frequencies of unique barcodes in each bacterial population from different sites are shown. (A) Inoculum samples. Barcode frequency was analyzed in the 26 bacterial aliquots that were each used to inoculate a different mouse in the STAMP experiment. Six representative frequency distributions are shown. (B-D) Barcode frequency distributions after noise removal for the output samples from mice sacrificed at (B) 24, (C) 48 or (D) 72 hours post-orogastric gavage. Each dot represents the frequency at which one specific barcode was detected. For each mouse ("M#"), dots representing the most frequent clones identified in the stomach are colored blue in all organs, and dots representing the most frequent clones identified in the small intestine are colored red.